Cape Peninsula
University of Technology

Mechanical properties of friction stir welded dissimilar aluminium alloys (1050 and 5083 aluminium alloy plates)

by

Nontle Mbana

Thesis submitted in fulfilment of the requirements for the degree

Master of Engineering: Mechanical Engineering

in the Faculty of Engineering

at the Cape Peninsula University of Technology

Supervisor: Dr V Msomi

Bellville Campus

06 September 2019

Declaration

I, Nontle Mbana, declare that the contents of this dissertation/thesis represent my own unaided work, and that the dissertation/thesis has not previously been submitted for academic examination towards any qualification. Furthermore, it represents my own opinions and not necessarily those of the Cape Peninsula University of Technology.

N Mbana	06 September 2019
Signed	Date

Abstract

Friction stir welding is a solid-state joining process. This welding technique is energy efficient and environmentally friendly. It is also categorized as the best welding technique when compared to other conventional welding techniques. FSW does not face problems faced by the other conventional welding techniques like the solidification process, the loss of alloying elements, the presence of segregation, porosities, blowhole and cracks formed in the weld joint. It can also be used to join high strength aerospace aluminium alloys and other metallic alloys that are hard to weld by conventional welding. Friction stir welding is considered to be the most important development in the welding of aluminium alloys. Generally, the mechanical properties of conventionally welded aluminium joints are poor and not attractive.

This study reports on the analysis of the mechanical properties of the friction stir welded dissimilar aluminium alloys (1050-H14 and 5083-H111). The study was conducted using 6 mm thick 1050-H14 and 5083-H111 aluminium alloy plates which were cut to fit the friction stir welding machine. The profile of the pin was triangular threaded with 20 mm shoulder diameter and 6 mm pin diameter. The triangular threaded pin had 1mm pitch and the height of 5.8 mm. The FSW parameters were chosen using Taguchi method. The rotational speed and transverse that was set during the test was 1000 rpm and 30 mm/min respectively. Tool tilting angle used during all the tests was kept constant at 2 degrees. Computerized numerical control (CNC) wire cutter was used to cut the specimens. This type of cutting was selected because it does not introduce heat during cutting and to ensure that the microstructure integrity is maintained.

The microstructure and mechanical properties of the joints were studied using tensile test, bending test, optical microscope, scanning electron microscope (SEM) and microshardness test. The tensile test results showed that the ultimate tensile strength (UTS) of AA5083 parent material is higher than the one of the welded joint. It was also noticed that all tensile test specimens fractured on advancing side (AA1050). The bending results presented good ductility, allowing for very high bend angles and no cracks were observed. The bending load was applied at the center of the specimens but the bending of all the specimens was on the side of AA1050. There was a variation in grain size between AA1050 and AA5083 parent materials where AA1050 had higher grain sizes while AA5083 had smaller grain sizes. The grain size for the base metal AA1050 was ranging between 25 – 33 µm while the grain size for AA5083 base metal ranged between 6.6 – 8 µm. The grain size for the stir zone or welded region ranged between 7.3-11.4 µm. The fracture of the tensile test specimens was also investigated through SEM. All the specimens show a cup like dimpled fracture which is

a characterization of ductile failure mode. The microhardness of AA1050 base material is about 40 while the one for AA5083 base material ranges around 80. There is notable decrease in microhardness from the AA5083 side towards the center which then followed by the notable drastic increase towards the center of the weld.

Acknowledgements

I would like to thank God for giving this opportunity because I know without Him I wouldn't be where I am today. My deepest gratitude goes to Dr Msomi, my supervisor, my mentor for his continuous encouragement and guidance. He has walked me through all the stages of the experiment as well as the writing of this thesis. Without his guidance, experiments and this thesis could not have finished. Secondly, I would like to thank Mr Moni for supporting us and making sure that we have everything that we need from materials to the machines. Not forgetting my fellow colleagues who gave me their help and time in listening to me and helping me work out my problems during the difficult part of the thesis. Lastly, my thanks would go to my beloved family and my husband for their support, loving, considerations and great confidence in me through these years.

Contents

List of Figures

List of tables

Appendices

Abbreviations

AA	Aluminium alloy
AS	Advancing side
ASTM	American Society of Testing and Materials.
AZ	Affected Zone
BHF	Blank holding force
BM/PM	Base material/ Parent Material
CNC	Computerized Numerical Control
Cu	Copper
Fe	Iron
FSP	Friction Stir Processing
FSW	Friction stir welding
HAZ	Heat affected zone
HCL	Hydrochloric acid
HF	Hydrofluoric acid
HNO3	Nitric acid
H2O	Water
Mg	Magnesium
Mn	Manganese
MIG	Metal Inert Gas
PD	Plunge Pepth
PFZ	Precipitate-Free Zone
PP	Pin Profile
RS	Retreating Side
SD	Shoulder Diameter
SEM	Scanning Electron Microscopy
Si	Silicon
TEM	Transmission Electron Microscope
TMAZ	Thermo-Mechanically Affected Zone
Ti	Titanium
TRS	Tool Rotation Speed
TWI	The Welding Institute
TIG	Tungsten Inert Gas
UTS	Ultimate Tensile Strength
WN/NZ	Weld Nugget/ Nugget Zone
WS	Welding Speed
YS	Yield Strength

CHAPTER ONE

INTRODUCTION

1.1. Introduction

Friction stir welding (FSW) is a solid-state joining process that uses a non-consumable rotational tool to join two plates without melting the material. Heat is generated by friction between the rotating tool and the workpieces which leads to a softened region close to the FSW tool. While the tool is traversing along the joint line, it mechanically mixes the two workpieces and forges the hot and softened metal by the mechanical pressure [Mishra & Mahoney, 2007].

Friction stir welding was initially invented to join aluminium alloys which were very difficult to weld using the conventional methods. Aluminium alloys are mostly used in many industries like aviation, shipbuilding and automotive because of their lightweight. FSW can also join other materials like copper and its alloys, titanium and magnesium and its alloys [Thomas & Nicholas, 1997]. When the aluminium alloys are welded with the conventional technique, they are likely to have weld splitting on the joint line. Also, fusion welding of aluminium alloys is difficult than the welding of steel due to their low melting point, softness, and so forth. The aluminium alloys are sometimes bent and shrink when conventional welding is used due to residual thermal stress [Genevois et al., 2005].

FSW does not melt any parent material and it produces a strong welding joint. FSW is known to have the best metallurgical properties when compared to fusion welding and this is caused by the microstructural modification which occurs during welding. Mishra & Ma (2005) reported that to have a great weld and to avoid defect on the weld it is important to take welding parameters, material flow and heat generation into consideration during the welding process.

Figure 1.1 shows the four important FSW steps i.e. plunging, dwelling, welding, and pulling. The tool is inserted into the butt joint slowly until the shoulder touches the surface of the workpieces. Then, the tool is forced by the machine to maintain contact between the shoulder and the surface of the sheet. This downward force creates frictional heat between the shoulder, the pin, and the workpieces, which almost reaches 80% of the melting point. The tool travels along the welding direction through the lateral force that is coming from the welding machine. That lateral motion caused by the lateral force is called travel speed [Farias et al., 2013]

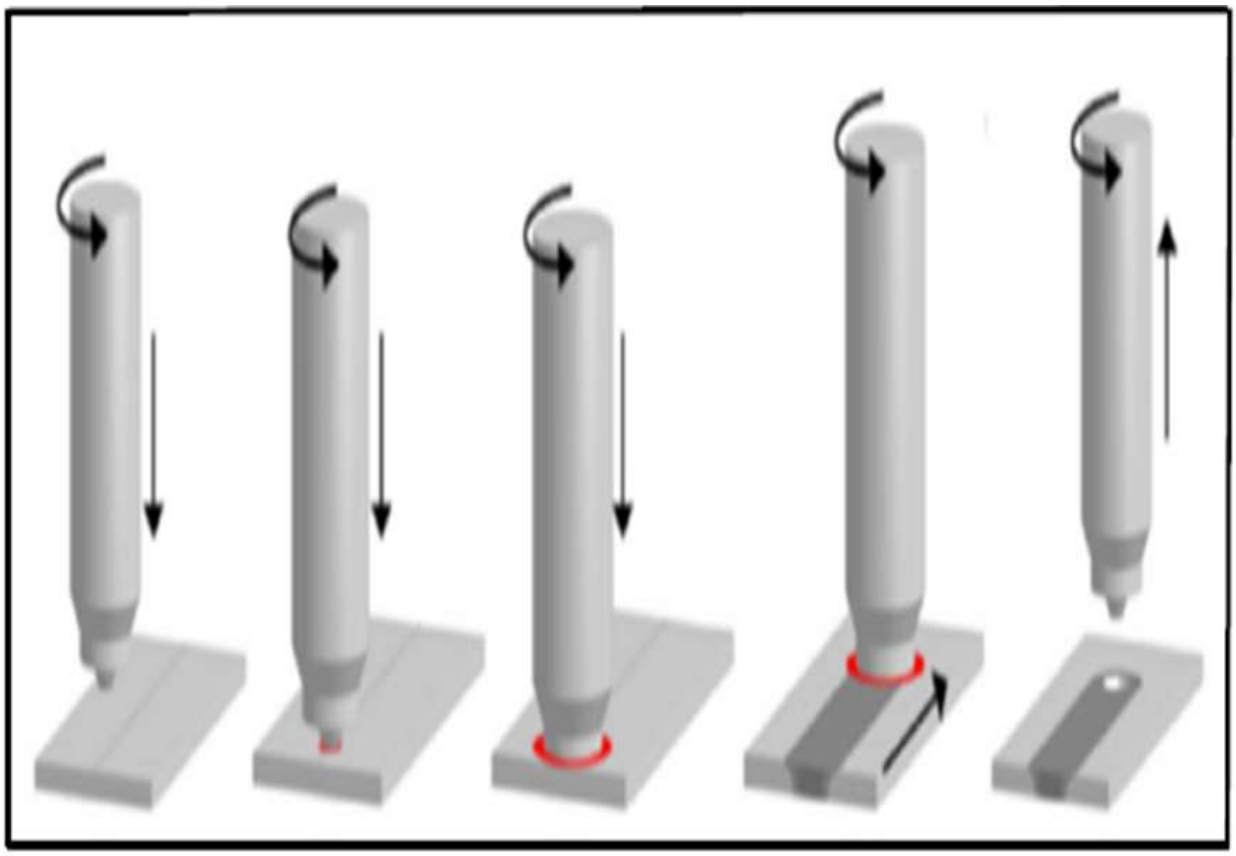

Figure 1.1: The friction stir welding process steps [Farias et al., 2013]

A rotating tool is pushed against the surface of two adjoining or overlapping plates as illustrated in figure 1.2. The side of the weld where the tool rotation is the same as the tool travel direction is called advancing side, and where the tool rotation is opposite the tool travel direction is known as a retreating side. An essential component of the tool is the pin

which protrudes from the shoulder, and its length is slightly less than the thickness of the plate.

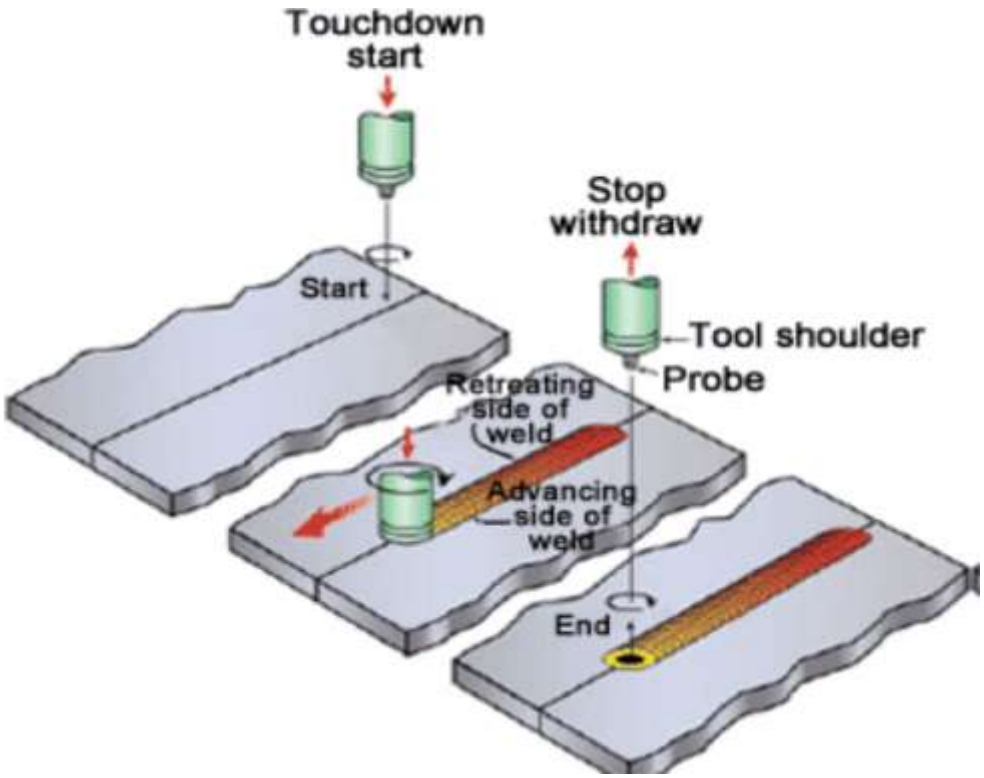

Figure 1.2: Schematic diagram of the FSW process [Tiwari et al., 2013]

The shearing activity and the high pressure during the friction stir welding generate frictional heat. The frictional heat influences the plasticised zone of material to fit in with the test. When the tool traverses along the line of the joint it clears the material around the pin between the retreating side of the tool and the surrounding undeformed material. It then removed the material to form a solid joint behind the tool. The procedure is defined asymmetrical, as a large portion of the distorted material is expelled past the tool retreating side [Tiwari et al., 2013]. There is a lot of work that has been done under the subject of FSW and the majority of work include the welding of similar and dissimilar materials. The main focus of this study will be on using FSW technique to weld 1050 and 5083 dissimilar aluminium alloys.

AA5083 is known for excellent performance in extraordinary conditions. This grade holds excellent strength after welding and it has the highest strength of the non-heat treatable alloys. It is weldable, machinable and formable even in arc processes like TIG or MIG. This alloy is used in many applications like production of welded components for shipbuilding, railway, storage tank, piping, different panels, automotive, tubing, protection layer plates, and military vehicles. To obtain superplastic properties, aluminium alloys must be friction stir processed to have the best results of grain refinement [Klob et al., 2012].

Aluminium alloy 1050 is a common grade of aluminium for regular sheet metal work and also applied in the place where moderate strength is required. It is highly ductile, high reflective finish and is also known for its outstanding corrosion resistance. Aluminium alloy 1050 is normally used for containers of the food industry, chemical process plant equipment, pyrotechnic powder, architectural flashings, lamp reflectors and cable sheathing [Andalucia, 2013].

1.2. Problem statement

Lightweight vehicles have become very important in the automotive industries. Using lightweight materials such as aluminium alloys and other lightweight metals have become extremely important to transportation industries. More mass in a car means more power needed to speed up and keep them moving. However, reducing the mass not only reduces fuel consumption but also reduces carbon emissions. Lots of manufacturing industries are using lightweight material instead of steel to form a lighter and stronger structure, which lead to a greater emphasis on the improvement of joining processes to allow interlocking formed by the material itself instead of using rivets, bolts, adhesives, or any other mass addition.

FSW has become the new process that is replacing mechanical fasteners and other fusion welding techniques. It has become the best candidate for joining aluminium alloys because it does not melt the materials being welded rather softens them. The joining of aluminium alloys that are widely apart from each other remains the subject under investigation. This

study is aiming at analysing the joint of the aluminium alloys that are widely apart from each other, specifically 1050 and 5083.

1.3. Research Objectives

The aim of this study is to investigate the mechanical properties of the friction stir welded joint of 1050 and 5083 dissimilar aluminium alloys. This study, therefore, discusses findings from joining the two materials. Objectives of the research are as follows:

- Use FSW technique to weld 1050 and 5083 dissimilar aluminium alloys
- To investigate the quality of the joint and analyse the mechanical properties of the weld joint
- Compare the weld joint properties against parent materials

1.4. Background to research

Material selection on the development of the joining technique is one of the challenges in many industries. There are many industries which are focusing on developing new structures that are environmentally friendly. One of the industries that is focusing on reducing the weight of their products is the automotive industry. This industry is looking at reducing the weight of the cars but maintaining their performances. Most components of the cars are mainly produced from plastic and aluminium materials. The production of the component from aluminium suggests that the aluminium may be joined with other different material or different aluminium alloys be used in producing certain components. The joining of two or more different materials would require the joining technique that is relevant to the materials to be joined. Conventional welding of dissimilar welding such as aluminium is quite challenging due to differences in melting point and mechanical properties of the involved alloys. The process results in porosity and crack formation on the welded joint [Coelho et al., 2012].

The welding of aluminium alloys such as 2XXX and 7XXX series was extremely difficult before the invention of the friction stir welding process. It was hard to have high quality and crack free welds. These aluminium alloys were known as non-weldable due to the poor hardening microstructure and the presence of porosity in the welded joint. These alloys make the welded part of these alloys by ordinary welding procedure not attractive [Mishra and Ma, 2005]. Friction stir welding was invented to take care of these issues and make all aluminium alloys weldable.

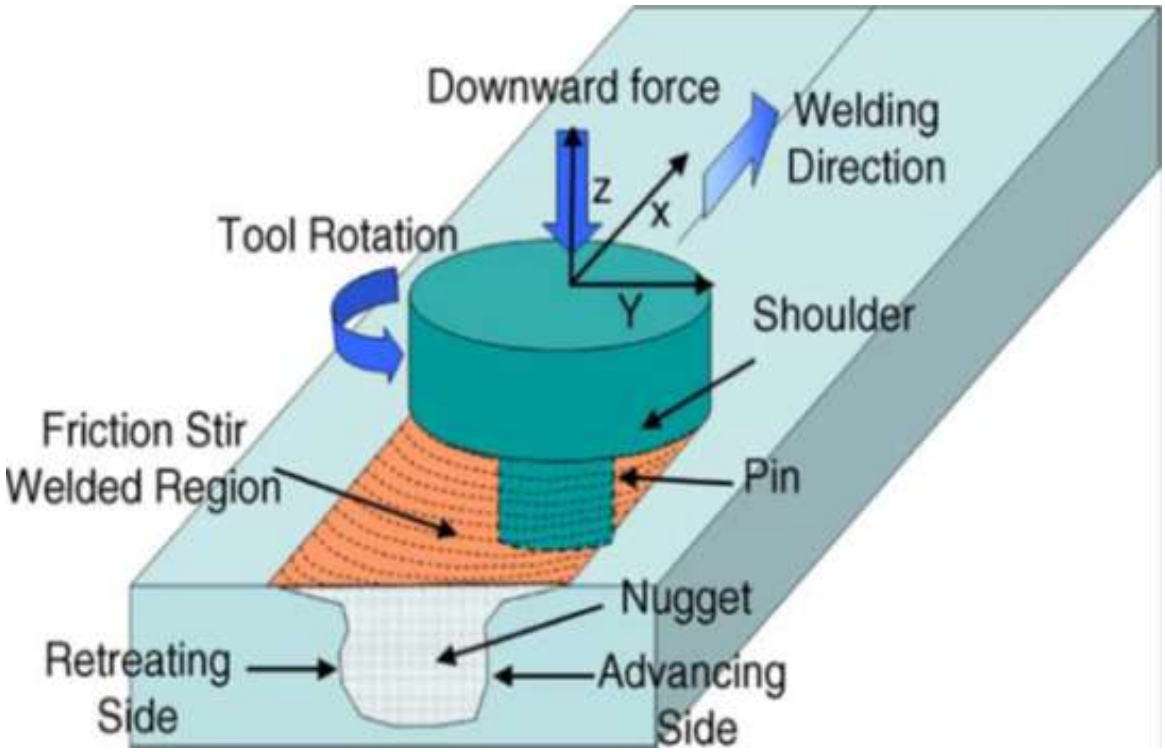

Figure 1.3: Schematic drawing of friction stir welding [Mishra and Ma, 2005]

FSW uses a non-consumable rotating tool to join two plates. The function of the tool is to heat the workpiece and move the material to produce the weld. The produced heat softens the material and the rotation of the tool moves the material from the front to the back of the pin [London, 2001]. FSW is the most important development welding technique in metal joining due to its energy efficiency. It consumes less energy as it does not use cover gas or flux. Therefore, any alloys can be welded without stressing over the compatibility of composition, which is an issue in conventional welding [Rhodes et al., 1997]

1.5. Related Literature

Welding dissimilar materials are quite challenging when compared with welding similar materials due to the difference in mechanical properties and chemical composition of the base materials. To acquire better weld mechanical properties, the harder material must be placed on the advancing side and softer material placed in the retreating side [Sadeesh et al., 2014].

FSW technique was developed to join similar aluminium plates but now can be employed to weld different materials (similar or dissimilar). Based on this capability, FSW has become a need of more than arc welding in industries. The aeronautics industry uses about 20% of aluminium in building flights. The objective of this industry was to use more than this percent of aluminium in building their flights due to weight to strength ratio, but it was not easy before the FSW was being developed. There are more chances that this percentage can be improved due to the arrival of FSW technique [Boşneag et al., 2017].

In as much as the analysis of welding dissimilar material is a subject of investigation, it was quite not clear on the impact of material's location towards the joints. Choi et al. (2010) critically analysed the effect of location variation in FSW of steel with different carbon content. It was discovered that the placement of stronger material on the advancing side reduces the weld nugget size and increases the amount of martensite formation. The location of the strongest material on the advancing side lead to higher temperature and stress due to the highest temperature on the advancing side.

The use of dissimilar materials to analyse different mechanical behaviour has been the work in progress. This involves the analysis of the strain hardening behaviour on the friction stir welded dissimilar alloys which are mechanical far apart from each other i.e. 2024-T351 and 5083-H112, 2024-T351 and 7075-T651 [Niu et al., 2018]. This analysis was performed on two types of joints i.e. 2024-T351 and 5083-H112 with 2024-T351 on the advancing side and 5083-H112 on the retreating side. The second joint was 2024-T351 and 7075-T651 with

2024-T351 on the retreating side and 7075-T651 on the advancing side. It was discovered that the strain-hardening rate of AA7075/AA2024 joint was higher than that of parent material while the strain-hardening rate of AA2024/AA5083 joint lies between those of parent material. It was also found that the tensile properties of both joints are lower than those of parent material.

Kumar and Kaila (2010) showed that this asymmetry can be important even for dissimilar aluminium alloys that have much higher thermal conductivity than steels. They compared the tensile strength and ductility of similar and dissimilar aluminium alloy FSW welds and showed that the position of the tool with respect to the original joint interface affects the strength and ductility of the joints. The optimal strength and ductility of the weld can be obtained only if the tool offset distance is optimised.

The microstructural analysis was studied correlatively with mechanical properties of the FSW joint using dissimilar alloys by Xia-wei et al. (2012). The lamellar structure in the bottom of the nugget zone was found to be more homogeneous and finer than other regions. The hardness on the copper side of the nugget was higher than that on the aluminium side. The UTS and the elongation of the dissimilar alloys were found to be 152 MPa and 6.3% respectively, and the dissimilar joint failed in a ductile-brittle fracture mode.

1.6. Organization of the dissertation

This dissertation is organized as follows

Chapter 1 – Introduction

This chapter gives a brief introduction about friction stir welding, related literature, problem statement and background of the study. Objectives of this study are also listed in this chapter.

Chapter 2 – Literature Review

This chapter explains a detailed literature review between FSW of similar and dissimilar alloys. It also explains process parameters and their importance in the process.

Chapter 3 – Experimental setup and performances

Equipment used for the welding and analysis of specimens, as well as welding preparation and performances is explained in this chapter. This chapter further analyses the mechanical and microstructural of the joints.

Chapter 4 –Test Results and Discussions

This chapter discusses the results obtained during analysis of the joints and parent material.

Chapter 5 – Conclusions

This chapter concludes based on results that were achieved on this study and also gives recommendations for future work.

CHAPTER TWO

LITERATURE REVIEW

2.1. Introduction

This chapter discusses a detailed literature review of friction stir welding process between similar and dissimilar aluminium alloys. It also explains other concepts that are related to the process, such as welding parameters and their importance to the process.

2.2. Friction stir welding of similar aluminium alloys

Before the invention of FSW technique, welding of aluminium alloys became a challenge due to limited welding techniques. Although metal inert gas (MIG) and tungsten inert gas(TIG) was already existing, the process couldn't weld some of the aluminium alloys. The main problems of TIG and MIG are the creation of porosity and hot cracking because of both the ingress of the oxygen and the impact of too much strain at the welded joint, which resulted from the melting and solidification process [Mathers, 2002].

The joining of aluminium alloys through conventional welding methods has been characterized by poor solidification microstructure, the high volume fraction of porosity in the fusion zone and the potential for segregation of alloying elements. These microstructural changes would lead to a significant loss in mechanical properties. Techniques such as spot resistance welds have been suggested, however, the high cost of surface preparation has not made this method a replacement for mechanical joining [Kostrivas, 1999]. As mechanical joints add weight to assemblies, research into alternative joining methods was of interest.

Kumbhar & Bhanumurthy (2012) did a comparative study on friction stir welding of similar to dissimilar aluminium alloys i.e. AA5052 to AA6061 and AA6061 to AA6061. The similar and dissimilar joints were produced at various combinations of tool rotation speeds and tool traverse speeds. The microstructural analysis reveals that there was no rigorous mixing in

the nugget region for both materials. The tensile properties of dissimilar material (AA5052-AA6061) were much improved than properties of similar materials (AA6061-AA6061).

Thomas et al. (2003) investigated this new joining innovation, friction stir welding. It was found that the process can be used to weld all aluminium alloys and surface oxide shows no inconvenience to the strategy. Based on the results of this investigation, it was recommended that the number of lightweight materials appropriate for the car, rail, marine and aviation transportation businesses can be made by FSW.

2.2.1. Tensile properties

Tensile behaviour of friction stir welded AA 6061-T4 joints was studied by Heidarzadeh et al. (2012). UTS of all joints was found to be lower than that of parent material in all tested rotational speed. However, increasing rotational speed, welding and axial force result in increase in UTS of the joint up until 159 MPa. Defect in the welded zone was observed due to lower rotational speed, higher welding speeds and lower axial forces, which resulted in poor plastic flow. Lim et al. (2004) also studied tensile behaviour of friction stir welded Al 6061-T651. The highest UTS of 250 MPa was achieved at the rotational speed and welding speed of 2500 rpm and 40 mm/min respectively. Although this strength was the highest, it was found to be lower than that of the parent material.

Thimmaraju et al. (2016) compared the microstructure and mechanical properties of friction stir welding of 6082 aluminium alloy using different tool profiles. Tensile properties were found to be varying with the change of tool. The highest tensile strength of 116.75 MPa was achieved on the joint made by hexagonal tool profile and the lowest tensile strength of 72.73 MPa was found on the joint made by triangle tool profile. The joint made by hexagonal tool profile fractured on the stir zone whereas the fracture was observed on the TMAZ region on the joint made by triangle tool profile.

2.2.2. Bending stress

Duong and Tran (2015) investigated the effects of friction stir welding parameters on bending behaviour of AA7075-T6. The results show that the parent material is brittle and cracked when reaches the bending strength of 701.22 MPa at the angle of 70^0. Most of the welded specimens broke at the small angle of bending due to heat input that was not enough to soften the parent material. Based on these results, it was concluded that process parameter of 800 rpm and 80 mm/min fabricated the best bending behaviour since it produces the bending strength of 796 MPa which is higher than that of parent material at the angle of 90^0.

Xu et al. (2009) conducted a study on Microstructure and mechanical properties of friction stir welded joints on AA2219-T6 using different rotational speed from 800rpm to 1300rpm and welding speed of 100 mm/min to 140 mm/min. The results showed no surface cracks or defect on the face bend test. Cracked were revealed on the root bend test between the weld nugget zone and TMAZ of all tested joints. The maximum bending force (F_{bb}) of 3.6 kN was reached at the angle of 80^0 on the defect-free weld. The minimum bending force of 1.98 kN at the angle of 25^0 was achieved due to flaws that were present in the joints.

2.2.3. Microstructural analysis

Ahmed et al. (2017) studied friction stir welding of similar and dissimilar AA7075 and AA5083. The constant rotation rate of 300 rpm and different traverse speeds of 50,100, 150, and 200 mm/min were used for this study. The microstructure of AA7075 joint showed a significant grain refining in the nugget zone with an average grain size of 6 µm when using traverse speed of 50 mm/min. When the welding speed was increased to 200 mm/min the average grain size was reduced to 2 µm. Further investigation was performed on similar friction stir welded of AA5083. A recrystallized coarser grain structure was obtained in AA5083 joints with an average grain size of 9 µm at 50 mm/min. When welding speed was increased to 200 mm/min, the average grain size was reduced to 3 µm. Based on these

results, it was concluded that the starting material characteristics have a significant impact on the final grain structure after friction stir welding.

Fazilah et al. (2016) did a study of Friction Stir Welding of Similar and Dissimilar Aluminium Alloys for Automotive Applications. The focus of the study was the investigation of the microstructure of FSW of AA5083 to AA5083. The onion ring was clearly identified in the stir zone due to material flow during the process. The investigation also reveals that the material was greatly deformed in thermo-mechanical affected zone (TMAZ) from the retreating side towards stir zone. The material from the advancing side also deformed but bent towards stir zone.

2.2.4. Scanning electron microscope (SEM)

Ji et al. (2014) investigated the formation and mechanical properties of stationary shoulder friction stir welded 6005A-T6 aluminium alloy, using the constant rotational speed of 2000 rpm and different welding speed. The fracture surface morphology of the joint fabricated with welding speed of 400 mm/min showed a large number of dimples and ductile fracture. The smaller dimples were revealed when the welding speed of 200 mm/min were utilised. Based on these findings, it was concluded that 400 mm/min is the best welding speed for the rotational speed of 2000 rpm. Therefore, the welding speed of 400 mm/min is the best for the ductility of the joint and welding speed of 200 mm/min is the worst. This agrees with the statement that says, “the higher the elongation of the joint, the better the ductility of the joint is” [Mishra and Ma, 2005].

Xu et al. (2009) further investigated the nature of fracture on the tensile test specimen on their study of microstructure and mechanical properties of friction stir welded joints on AA2219-T6. Different rotational speed and constant welding speed of 120 mm/min were utilised for this investigation. Different kinds of dimples were observed due to various rotational speeds. Deep-hole type dimples were observed at a rotational speed of 800, 900,

and 1100 rpm. Whereas shallow-hole type dimples were observed on the fracture fabricated at 1300 rpm. These results show that most of the failure resulted in a ductile-brittle fracture.

2.3. FSW of dissimilar materials

The joining of dissimilar materials poses an increased challenge. These materials have very different chemical compositions and physical properties. The incompatibility of these properties (melting point, thermal conductivity, thermal expansion, ductility, fatigue, elasticity modulus, etc.) can bring some difficulties during the joining process and subsequent product utilization. To succeed in joining these materials, it is necessary to overcome all these issues.

Tiwari et al. (2013) did a review on the FSW of aluminium alloy. On their investigation, they discovered that for the production of the good weld, the tool geometry is very important. It was also reported that welding parameters including rotation speed, traverse speed, tool tilt angle and plunged depth is very critical to produce sound and defect-free weld. Plunge depth has been found to be a critical parameter in the heat generation and for proper consolidation of material without defects. The plunge depth affects the force required during the plunging operation [Soundarajan et al., 2007].

Ewuola et al. (2015) investigated the effect of plunge depth on weld integrity of friction stir welds of dissimilar aluminium and copper. It was observed that the sizes of the surface areas of the voids vary with the plunge depth. An increase in the plunge depth resulted in a decrease in the surface area of the defects. The micrograph showed a better flow for both the copper and aluminium alloys at the higher plunge depth than the lower plunge depth. It was proposed that the higher plunge depth benefits from a higher vertical force of the tool, resulting in better material flow.

In most cases, the welding of dissimilar materials involves the welding of aluminium alloys which are not far from each in terms of mechanical properties i.e. 5xxx will be welded together with 6xxx, 6xxx welded with 7xxx. Recently, there attempts that have been made in

trying to weld the aluminium alloys that are mechanically far apart from each other i.e. FSW of AA2024 to AA6061 [Hou et al. 2018]. This investigation has used single and dual pin tool. The defect-free joint was obtained in all selected parameters produced by dual pin whereas single pin joints defect was found at the welding speed higher than 90 mm/min. Also, onion ring on the nugget region was visible with the dual-pin tool but it was absent on the single pin tool. The highest UTS of 242 MPa was obtained with the dual-pin tool at a welding speed of 150 mm/min, while single-pin the UTS of 173 MPa was obtained at a welding speed of 90 mm/min.

2.3.1. Tensile properties

Khodir & Shibayanagi (2008) did a study on the friction stir welding of AA2024T3 with AA7075T6 using a constant rotational speed of 20revs/s and different welding speed. All tensile tested specimens fractured on HAZ of AA2024T3 irrespective of welding parameters and which material was placed on the advancing side. The maximum tensile strength of 423 MPa which is 8% lower than the base material of AA2024T3 and 29% lower than the base material of AA7075T6 was achieved for the joint fabricated at the welding speed of 1.7mm/s and when the AA2024T4 is located on the advancing side. The lowest tensile strength of 381 MPa which is 17% lower than the base material AA2024T3 and 36% lower than the base material of AA7075T6 was achieved for the joint fabricated by the same welding speed of 1.7mm/s and when the AA7075T4 is located on the advancing side. Putting AA2024T3 on the retreating side led to reduction of tensile properties due to the occurrence of defect (kissing bond) on the root of the joint.

Ilangovan et al. (2015) did a study on the effect of tool pin profile on microstructure and tensile properties of friction stir welded dissimilar AA6061 and AA5086 aluminium alloy joints. AA6061 was placed on the advancing side while AA5086 was on the retreating side. A higher tensile strength of 169 MPa was achieved on the joint made by threaded cylindrical pin profiled tool. A lowest tensile strength of 126 MPa, which is 51.54% lower than the parent material of AA6061, and 40.57% lower than parent material of AA5086 was achieved on the

joint made by straight cylindrical pin profiled tool. The joint made by taper cylindrical pin profiled tool results in tensile strength of 163 MPa which is 35% and 20.29% lower than those of the parent material AA 6061 and AA 5086, respectively. Based on the results it was concluded that the threaded cylindrical pin profiled tool is the best tool profile for dissimilar alloys.

Guo et al. (2014) also investigated the effect of material location on the tensile property of the joint of AA6061 to AA7075 using a variety of different process parameters. In this investigation, all joint fractured on the heat-affected zone on the AA6061 side during tensile testing regardless of which material were located on the advancing side. They also found that when decreasing heat input, the tensile strength of dissimilar joint increases. The highest UTS of 245 MPa was obtained when AA6061 was located on the advancing side using welding and rotational speed of 5 mm/min and 1200 rpm respectively. Also, Silva et al. (2011) on their study of material flow and mechanical behaviour of dissimilar AA2024-T3 and AA7075-T6 aluminium alloys friction stir welds and Amancio-Filho et al. (2008) on the preliminary study on the microstructure and mechanical properties of dissimilar friction stir welds in aircraft aluminium alloys 2024-T351 and 6056-T4 both observed the same behaviour of fracture. Tensile test specimen fractured on the heat affected zone of the weaker material which is on AA2024 for both studies.

Kopyściański et al. (2016) did the analysis of friction stir welding of dissimilar aluminium alloy plates of 2017A-T451 and 7075-T651 with 6 mm thickness at a different tool rotation speed. This study was intending at determining the conditions that produce the highest weld quality. It was found that the highest UTS (406 MPa) was achieved when 2017A-T451 was on the advancing side. It was also established that the material that was located on the advancing side dominate on the weld centre. Ranjith & Kumar (2014) analysed the impact of joining two dissimilar aluminium alloys AA2014 T651 and AA6063 T651 by friction stir welding. It was discovered that the tensile strength was better when the tool was offset towards AA2014 (advancing side). When it was offset towards AA6063 (retreating side), it resulted in

insufficient heat generation on the advancing side. This lead to incomplete fusion of AA2014. Yadav (2015) investigated FSW of Dissimilar Aluminium alloys between AA1100 and AA6101-T6 using welding parameters of 1500 rpm and 3 mm/min. Tensile strength of the joint was found to be 153.33 MPa, which was less than both parent materials but very close to the weaker material (AA1100).

2.3.2. Bending stress

Ravikumar et al. (2013) evaluated the bending strength for dissimilar friction stir welded AA6061 T651 - AA7075 T651 butt joint using varying process parameters and different tool profile such as taper cylindrical threaded, taper square threaded and simple square. AA6061 T651 was placed on the advancing side while AA7075 T651 was on the retreating side. Tunnel hole defect was observed in all joint. All tested specimen bend on the advancing side of AA6061 T651.The highest bending strength of 0.039 N/mm^2 was achieved on the joints made by taper cylindrical threaded tool profile. The lowest bending strength of 0.018 N/mm^2 was achieved on the joint made by simple square tool. The joint made by taper square threaded resulted in bending stress of 0.021 N/mm^2. Based on those results, it was concluded that taper cylindrical threaded tool profile found to withstands high ultimate load and best tool since it revealed good bending strength compared to the other two.

Moreira et al. (2009) conducted a study on mechanical and metallurgical characterization of friction stir welding joints of dissimilar AA6061-T6 with AA6082-T6 using welding parameters of 1120 rpm and 224 mm/min respectively. The bending test results showed no defects or root flaws on the welded joint. This study reveals that there was a linear behaviour in both parent materials until it reaches a load of 420 N. It was reported that the welded joints of AA6061 to AA6062 also presented a linear behaviour but until it reaches the load of 220 N.

2.3.3. Microstructural analysis

Guo et al. (2014) investigated the effect of material positioning on friction stir welding of dissimilar AA6061 and AA7075. The study revealed that the material mixing is much more

effective when AA6061 was placed on the advancing side and multiple vortexes centres formed vertically in the nugget. Onion ring formation was also observed in joint.

Silva et al. (2011) studied the microstructure of dissimilar AA2024-T3 and AA7075-T6 friction stir weld. The microstructure on HAZ was found to be similar to that of the base material. Various rotational speeds were employed. Onion ring formation was observed due to proper material mixing at an optimum rotational speed of 2000 rpm. The grain size was found to be 5-7 µm in the 2024 region and 3-5 µm in the 7075 region. This behaviour agrees with the results of Tang et al.(1998) which discovered that the increase in heat input results in the best mixing patterns. Zhang et al. (2019) also followed a similar approach to their study of FSW of similar and dissimilar AA7075-T651 and AA2024-T351. They discovered that rotational speed has a remarkable influence on the proper mixing of the joint. Increasing rotational speed lead to widening the TMAZ on the advancing side and retreating side. The onion ring was also observed at a higher rotational speed of 1650 rpm but the average grain size of 1.7 µm occurred in all the joints at a lowest rotational speed of 600 rpm.

Fazilah et al. (2016) investigated the microstructure of dissimilar welded joints of AA5083 to AA6061. Stir zone was indicated by wavy and distorted pattern instead of onion ring, this was due to the different behaviour of aluminium alloys. The macrograph revealed the mixing of two materials in the stir zone. Based on these results, it was recommended that a simple threaded pin produced defect free weld when AA5083 is on the advancing side. Aval et al. (2011) also investigated the thermo-mechanical and microstructural issues in dissimilar friction stir welding of AA5086–AA6061. The study revealed that the mixing of the material in the stir zone was more efficient when AA5086 was placed on the advancing side. The microstructural studies also revealed that the finer grains were produced on the retreating side (AA6061) compared to the advancing side (AA5086).

2.3.4. SEM

The tensile test specimen fracture surfaces were further examined to analyse the factography of the AA6061 and AA7050 SEM on the study conducted by [Rodriguez et al., 2015]. The analysis revealed that the tensile test specimen failed through the heat affected zone of AA6061 side due to low heat tool rotational speed. Failure also occurred in the stir zone due to poor material intermixing. The fracture resulted in a ductile morphology represented by the formation of dimples.

Sarsılmaz et al. (2012) evaluated the microstructure and fatigue properties of dissimilar AA7075/AA6061 joints produced by friction stir welding. SEM observation was performed on the fractured surface of tensile tested specimens. SEM fractograph of the samples welded at 1400 rpm using triangular tool pin showed microvoid of different sizes. The fractured surface also showed a uniform and smaller ductile dimples at higher rotation and welding speed.

2.4. Welding parameters in friction stir welding

One advantage with friction stir welding is that the parameters can be controlled hence controlling the energy input to the system. The tool rotation speed (TRS) and the welding speed (WS) are the two most essential process parameters that influence the thermal history, material flow, microstructural evolution and the properties of the joint. The downforce applied parallel to the axis of rotation is another process parameter that influences heat generation. There are different elements that can influence the weld characteristics in the FSW process. This includes initially heat treatment condition of the workpiece, material type and hardness of the tool, material and thickness of the backing plate, type of cooling plan and the clamping fixture. Selection of friction stir welding parameters that deliver satisfactory mechanical, microstructural, fatigue and corrosion properties is an essential prerequisite to get productive, defects free friction stir welded joints [Serio et al., 2016].

The parameters that are very important for the friction stir welding process include the rotational speed (ω, rpm), where the direction can be either clockwise or counter clockwise. The second parameter is travel speed, which is measured along the line of the welding joint. Travel speed symbol and unit are v and mm/min, respectively. The third parameter is a tilt angle. A suitable tilt direction will guarantee that the tool shoulder holds the material by the threaded pin from the front to the back. Moreover, tilting the tool influences weld appearance and thinning. A suitable tilting angle for the friction stir welding tool is between 1-3º. The last welding parameter is the downward axial force of the tool shoulder on the workpiece that is applied by the machine [Cavaliere et al., 2007].

Meshram and Kodli (2014) showed that perfect welding by friction stir welding is very difficult because the heat generated by the friction depends on controlling the above four factors. Applying low rotational speeds and high axial pressure during friction stir welding produces a high rate of deformation, and this results in a short weld time. High rotational speed and low axial pressure produce a relatively low rate of deformation. The optimum friction time for welding two sheets during friction stir welding depends on many factors. These factors include dimensions, material composition, rotational speed and friction pressure. If the friction time is too short, the heating distribution will become irregular, and the bond strength will be weak in some regions. Moreover, when the heating time exceeds the optimum time, productivity will decrease while increasing material consumption. Material consumption leads to a coarse grain structure [Sengar and Kuma, 2012].

The most important part of the friction stir welding process is the tool geometry. FSW tool has two part which is shoulder and a pin, designing of these parts is a critical role for welding quality. The main functions of the tool are localized heating and material flow. The function of the pin is to deform the material around the tool and produce heat. Heat generation starts when the tool shoulder touches the workpiece. The shoulder is used to prevent material removal from the welding area and helps material to move around the tool. The plasticized material which is caught by the shoulder that moves along with the weld is extruded from the

main to the trailing side of the tool, this is done to create a smooth surface finish. The extra function of the tool is stirring and moving of material [Gharacheh, 2011].

The tool geometry and the procedure parameters influence the heat generation, material flow, microstructure evolution and the properties of the joint. The tool life relies upon the procedure parameters utilized. Mishra and Ma (2005) showed a detailed review on friction mix welding, a mechanism in charge of the formation of welds and microstructural refinement, and impacts of process parameters on resultant microstructure and final mechanical properties.

The tool geometry plays a very important role in welding dissimilar materials. Welding dissimilar alloys require the use of different tool profiles such as threaded, squared and triangular profiles to transfer the material from top of the joint to bottom and vice versa by stirring movement [Biswas & Kumar, 2011]. Kundu & Singh (2016) reported that tool pin profile geometry plays an important role in weld quality and also the surface quality on the weld joint depends upon the tool tilt angle. As the tool tilt angle increases, it gives less flow of semi-solid material.

Tool tilt angle is a parameter to improve the stuffing of the material by the tool shoulder. A suitable tilt angle of the rotating tool ensures that the shoulder of the tool holds the stirred material by tool pin and move material successfully from the front to the back of the pin. For aluminium welds, a tilt angle from 0° to 3° gives an incredible change in the microstructure development and material stream. A large tilt angle gives more firmly weld and uniform material flow [Joint, 2016].

2.5 Summary

It is clear from the literature that was included in this work that the use of FSW technique has been focusing on the welding of similar materials or alloys. There are also few attempts that were made in welding dissimilar alloys or materials but most of the dissimilar alloys are focusing on the dissimilar alloys that are not mechanically and chemically far from each

other. There are very few attempts that were made in welding alloys that are widely far apart and those studies used mostly 2xxx and 7xxx. There are no reports or works that dealt with the FSW on 1050 and 5083 dissimilar aluminium alloys hence the establishment of this study.

CHAPTER THREE

EXPERIMENTAL SETUP AND PERFORMANCE

This chapter consists of list of equipment used for welding as well as list of equipment used in analysis of the joints. The thorough explanation is given to each equipment. This chapter also analyses the mechanical and microstructural properties of the joint comparatively with base material.

3.1. The list of equipment used for the welding

The machines that were used in performing welding are listed below:

- Guillotine cutting machine
- Semi-automated milling machine

3.1.1. Guillotine cutting machine

Guillotine cutting machine is the machine that is used to cut the material using both foot and hand-powered technique (see figure 3.1 below). The machine consists of a shear table, gauging device, upper and lower blades. The shear table is used to rest the material while being sheared. The gauging device is used to measure the size of material that required and to ensure that the workpiece is cut where it needs to be. Upper and lower blades are for cutting the material.

Figure 3.1: Guillotine cutting machine

3.1.2. Semi-automated milling machine

The machine used to perform friction stir welding is a semi-automated milling machine that is shown in figure 3.2. The 141 mm wide by 700 mm long back plate (clamping fixture) was designed and inserted into the semi-automated milling machine bed. Other concepts that are related to the process such as FSW tool and clamps were also designed. The tool is used to produce the weld along the centre line of the workpieces. The backing plate is used to position the workpiece for clamping. Clamps are used to hold both backing plate and plate to be welded in position during welding.

Figure 3.2: Semi-automated milling machine

3.2. Welding preparation and performance

Dissimilar 1050 and 5083 aluminium alloys of 6 mm thick plates were cut into 70 mm X 530 mm (figure 3.3) using a guillotine machine in preparation for the friction stir welding technique. The plate dimensions were chosen to fit on the backing plate of 141 mm wide by 700 mm long. The vertical milling machine was used for the friction stir welding experiment.

Figure 3.3: Aluminium alloy plates

3.2.1. Experimental procedure

The two dissimilar plates were put on the semi-automated milling machine to be welded as shown in figure 3.4. AA5083 was kept on the retreating side throughout the experiments while AA1050 was on the advancing side due to the fact that the temperature is high on advancing side [Sundaram & Murugan, 2010]. The plates were fixed on the machine back plate by eight clamps. The function of clamps was to make sure the plates do not move apart when the rotating pin is in motion.

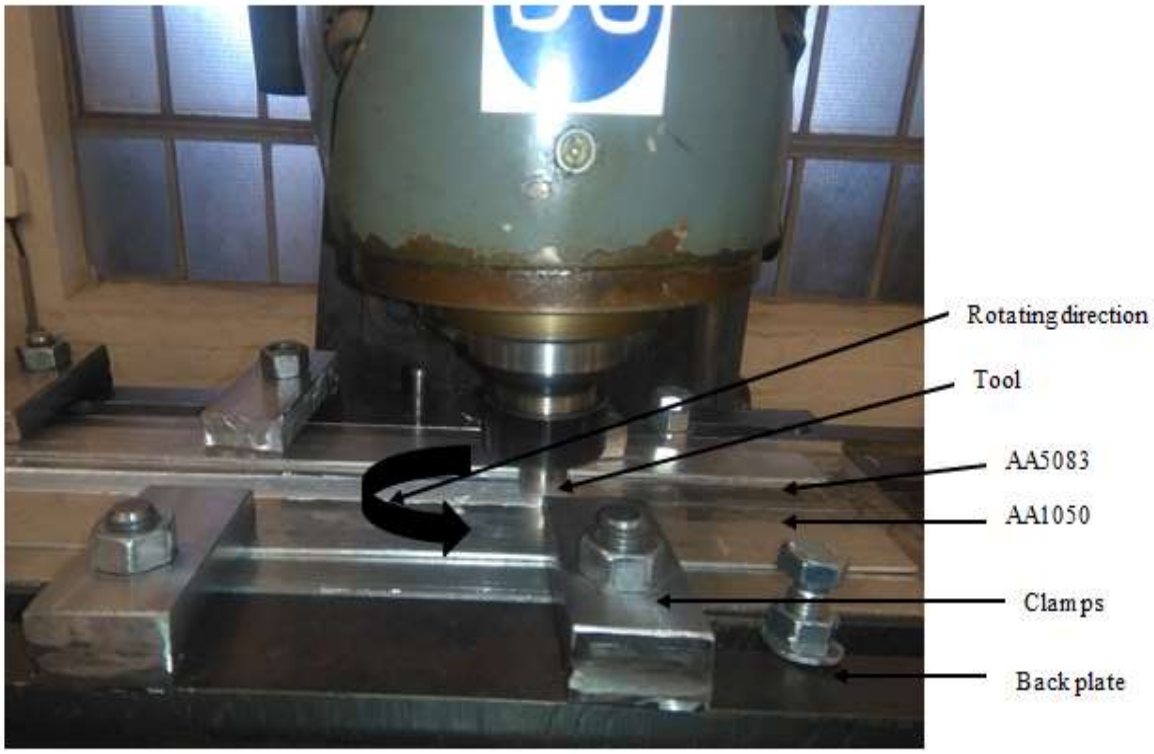

Figure 3.4: Semi-automated milling machine

The plates were then friction stir welded using high carbon steel (H13) tool (figure 3.5). The tool was machined using lathe machine and was heat treated to about 50HRB. The profile of the pin was triangular threaded with 20 mm shoulder diameter and 6 mm pin diameter. The triangular threaded pin had 1 mm pitch and the height of 5.8 mm. The FSW parameters were chosen using Taguchi method. The welding parameters are presented in table 3.1.

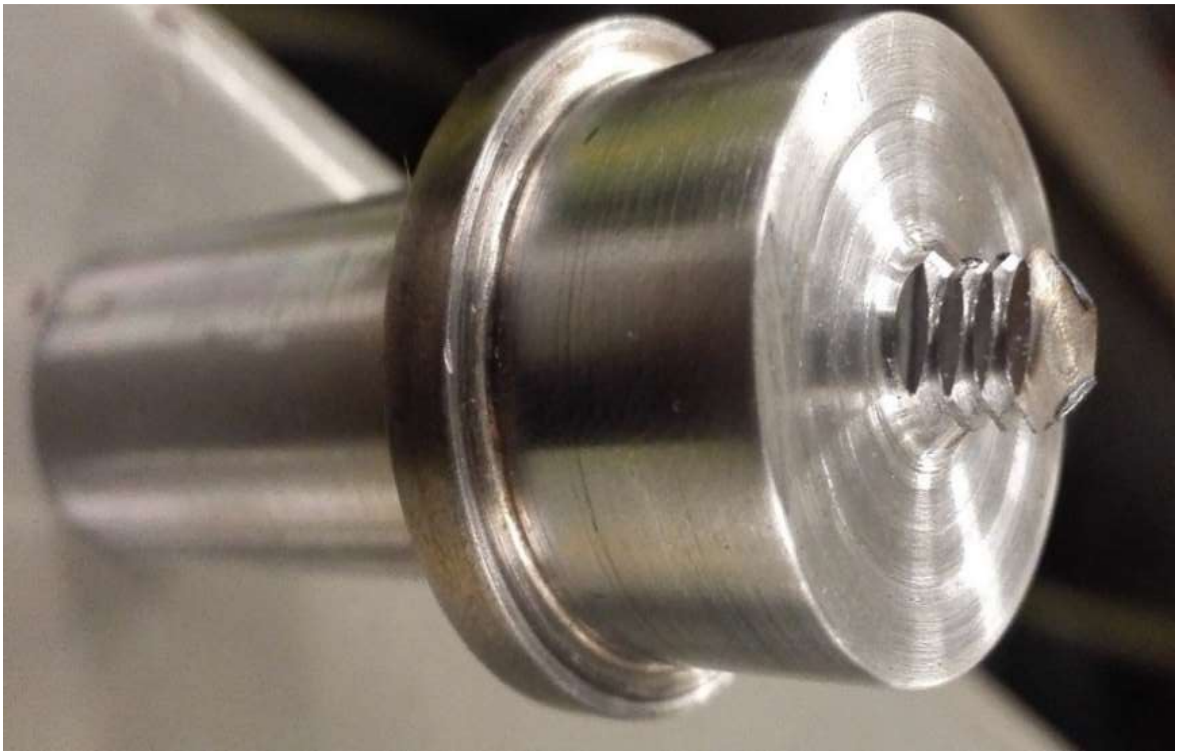

Figure 3.5: FSW tool

Table 3.1: Friction stir welding parameters.

Rotational speed (rpm)	Traverse speed (mm/min	Tilt angle (^{0})
1000	30	2

Figure 3.6 shows the start until the finish of the FSW process. Stage 1 shows two plates about to be welded together by means of friction stir welding. Stage 2 shows the initial point of the rotating pin. Stage 3 shows the welded part of the plates. Stage 4 shows the finished product of AA1050 and AA5083 aluminium welded plates. The FSW joint produced is presented in figure 3.7.

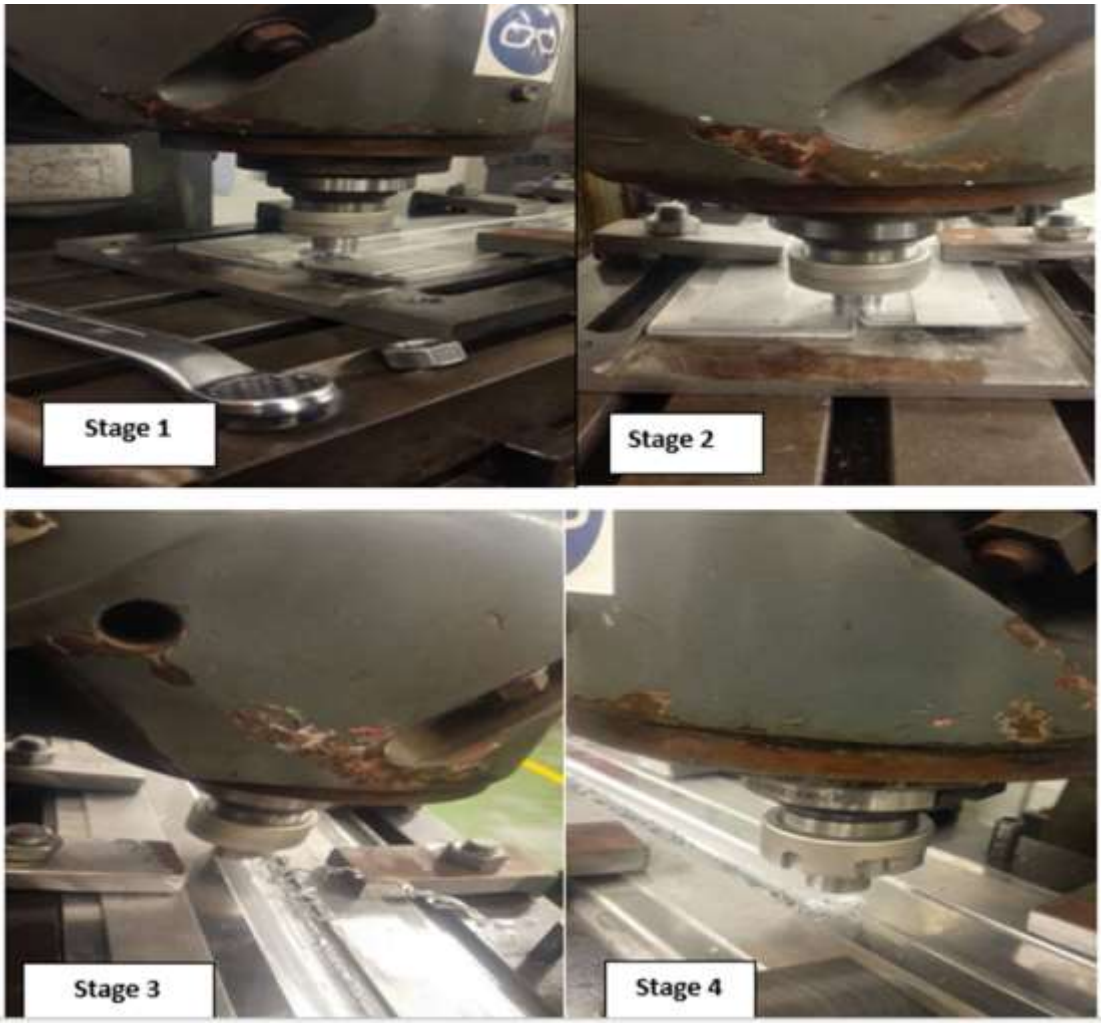

Figure 3.6: Friction stir welding process

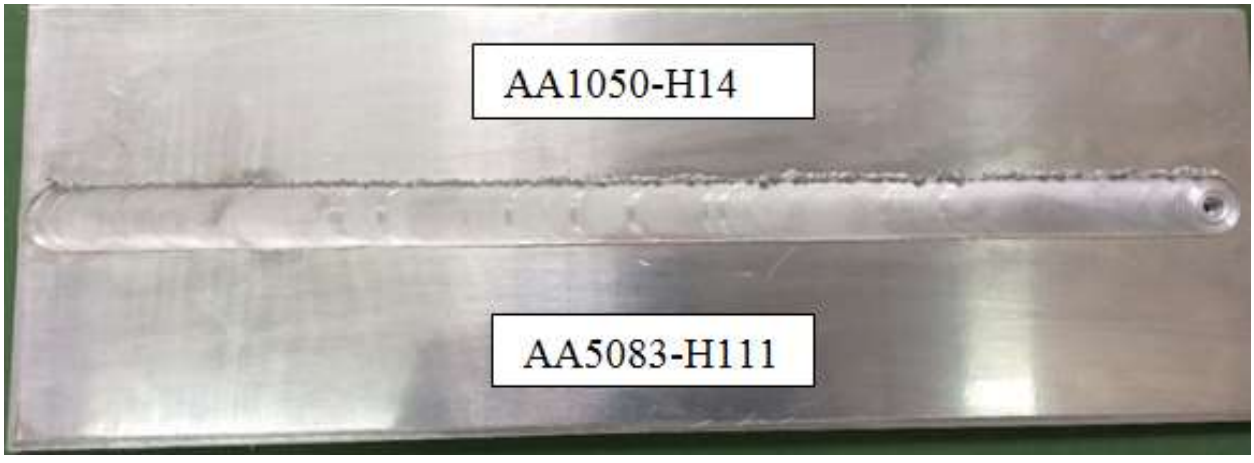

Figure 3.7: FSW plate

The next step followed the welding was to prepare the welded joint for different analysis and the next section discusses the procedure used in performing analysis and tests.

3.3. The list of equipment used for the analysis of specimens

The equipment that was used to analysed specimens is listed below:

- Wire cutter
- Mounting press machine
- Polishing machine
- Hounsfield Tensometer (Universal Testing Machine)
- Nikon Eclipse L150 microscope
- Zeiss Auriga Scanning electron microscope

3.3.1. Wire cutter

Wire cutter machine (figure 3.8) is a machine that is used for tool and die making. Wire (figure 3.9) is the main cutting tool in the wire cutter machine and the material of the wire can be brass, silver, copper, etc. The thickness of the wire ranges between 0.10 to 0.30 mm. High current is flowing through the wire and an electron is released from the wire and strike into the material. Spark is generated due to the electron strike on the material and the material burned out and cleaned by the deionized water running continuously. The machine was chosen because it introduces minimal heat during cutting.

Figure 3.8: Wire cutter

Figure 3.9: Electrical discharge wire

3.3.2 Mounting press machine

A Struers Labo-3 hot mounting press machine (see figure 3.10) is a machine where the specimen is placed in a cylinder together with the appropriate mounting resin. Antistick stearate powder is applied to the surface of the lower ram and upper ram to avoid sticking of resin. Specimens are placed on the ram with the surface to be viewed facing downwards. The ram is pressed down to its lower limit. Suitable amount of resin (about 1 scoop) is filled into the cylinder through the funnel. The top closure is placed with the upper ram on the mounting cylinder and be pressed down until its lower limit. The heating time, cooling time force and heating temperature are then set. The set parameters will then control the mounting until it is removed from the machine. The purpose of mounting the specimens is to protect fragile or coated materials during preparation and to obtain perfect edge holding.

Figure 3.10: Mounting press machine

3.3.3. Polishing machine

The Struers LaboPol-5 polishing machine (shown in figure 3.11) is a machine used for grinding metals, lapping and polishing using different consumables that are shown in figure 3.12. Preparation disc with suitable grit size is placed on the turntable. Then specimens are

also placed on the specimen holder. The running water is then switched on and the speed control gets adjusted between 50 – 500 rpm. The specimen gets polished until glossy.

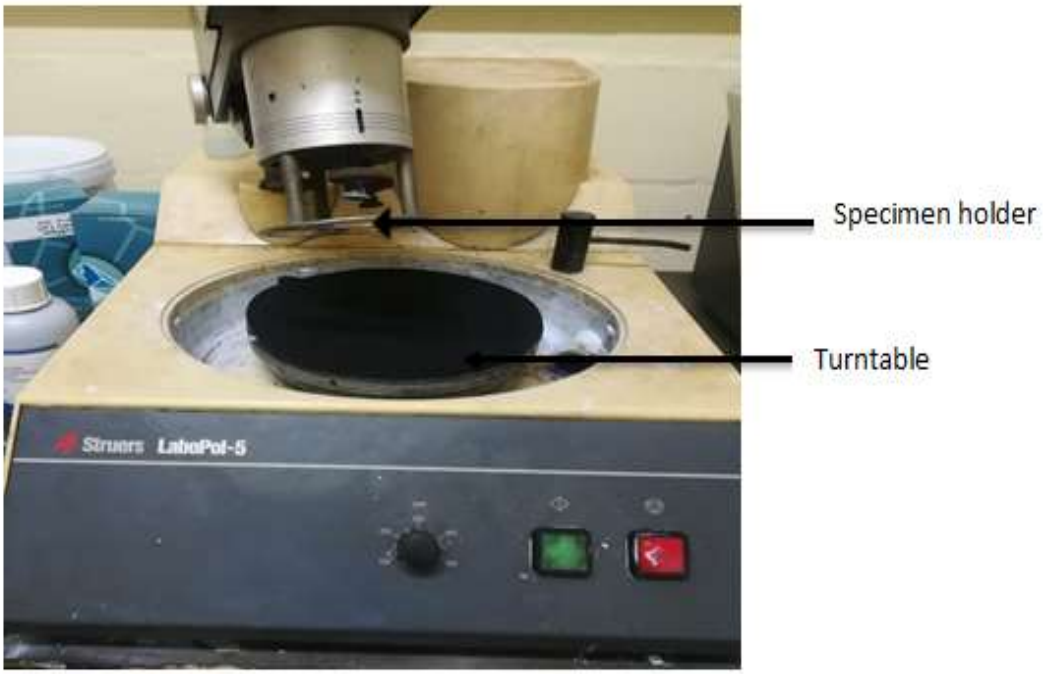

Figure 3.11: Polishing machine

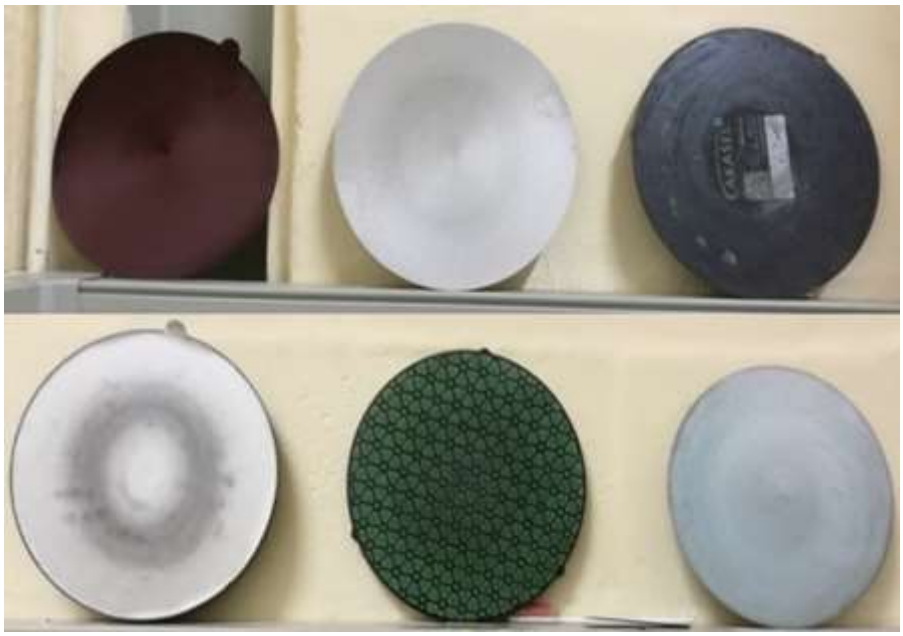

Figure 3.12: polishing discs

3.3.4. Hounsfield Tensometer (Universal Testing Machine)

Hounsfield tensometer is a machine that is used to do tensile tests. The data obtained from this machine is used to evaluate properties of material such as Young's modulus, tensile strength, etc. It is usually a universal testing machine loaded with the sample between two grips that are adjusted manually and automatically to apply force to the specimen. Material to be tested must be cut to a specific shape so as to fit the grips. In most cases, the dog bone shape is used. Specimen is normally inserted between two grips and the force is applied on opposite ends of the specimen until specimen breaks. The data recorded gets extracted for further processing.

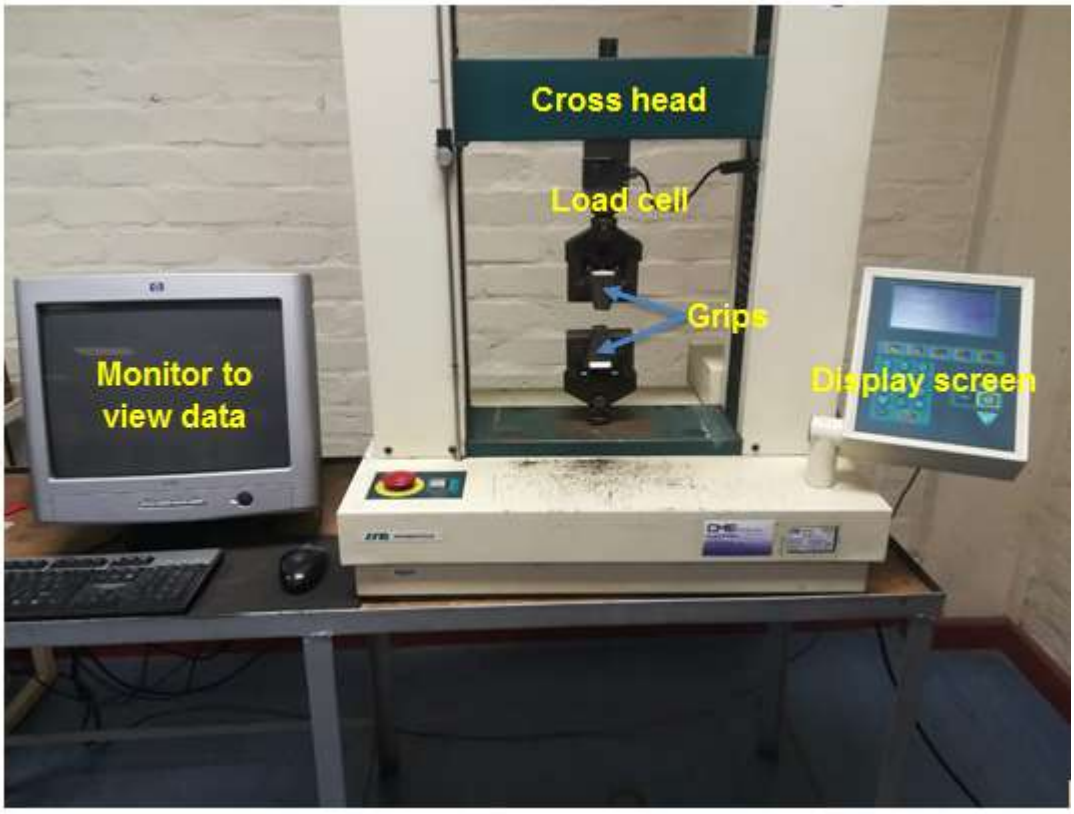

Figure 3.13: Hounsfield Tensometer

3.3.5. Nikon Eclipse L150 microscope

A microscope is an instrument that enlarges object that is too small to be seen. It produces an image in which the object appears larger. The photographs of cells that are taken using a microscope are called micrographs. The specimen is placed on top of the stage and be

exposed to light path through the use of knobs until the necessary focus is achieved. After obtaining approximately focus, the grain sizes are measured and the pictures are captured.

Figure 3.14: Nikon eclipse L150 microscope

3.3.6. Zeiss Auriga Scanning electron microscope analysis technique

Scanning electron microscopy (SEM) is an instrument that is used for inspecting topographies of specimens at very high magnifications. SEM inspection is often used in the analysis of die/package cracks and fracture surfaces, bond failures, and physical defects on the die or package surface. The general procedure for SEM is as follows: The samples are attached to a sample holder; they need to be electrically connected to the sample holder to prevent the electron beam from “charging” the sample and distorting the image. This is done through a double-sided conductive tape. A focused beam of electrons is scanned across the specimen to generate an image and analyse the specimen.

Figure 3.15: Zeiss Auriga Scanning electron microscope

3.4. Characterization and analysis

This section describes the mechanical and microstructural analysis of the welded joint. It should be noted that the friction stir welded joint had a start, middle and ending points. The specimens were all labelled A, B, and C. The ones labelled A, were cut at the beginning of the joint, the ones labelled B were cut in the middle of the joint and the ones labelled C were cut at the end of the joint. This format was followed throughout all the tests done. The tests performed are listed below:

The tests performed are listed below:

- Tensile test
- Microstructure test
- Bending test
- Scanning electron microscope (SEM)

- Microhardness test

3.4.1. Tensile Test

Prior to the performance of the tensile test, the specimens were cut from different locations of the welded plate as shown in figure 3.16. The dog-bone shaped specimens with dimensions shown in figure 3.17 were cut perpendicular to the weld joint. The wire cutter machine was used to cut these specimens and the E8M-04 standard was followed in cutting the specimens. The prepared specimens were then fixed to the Hounsfield tensile testing machine as shown in figure 3.18. The tensile parameters used for these tests are shown in Table 3.2. The data was logged and processed to produce the results that are presented in the next chapter.

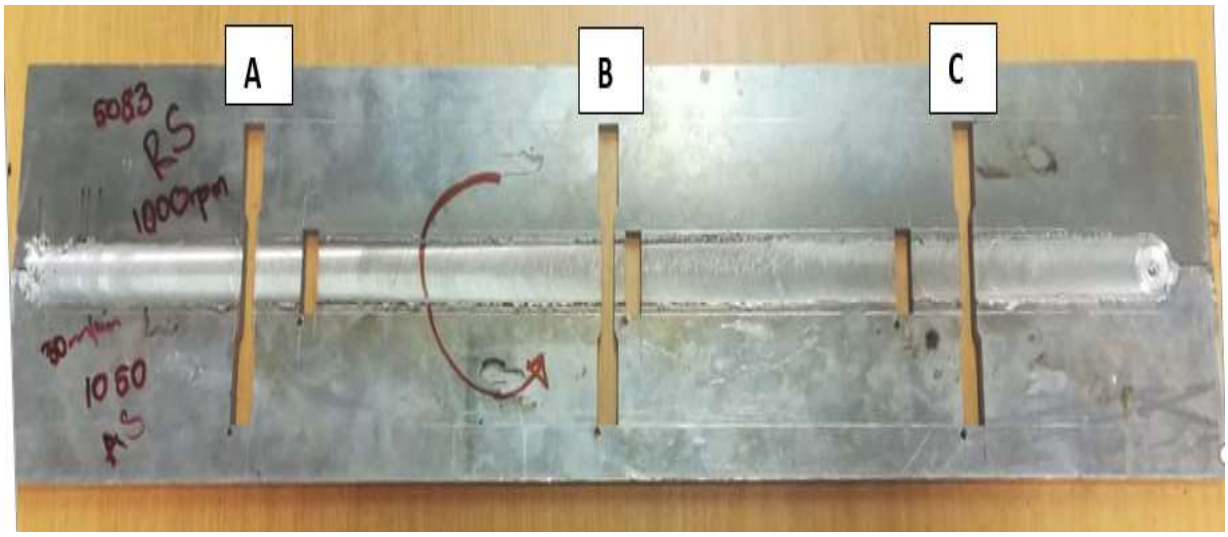

Figure 3.16: Frictions stir welding plate

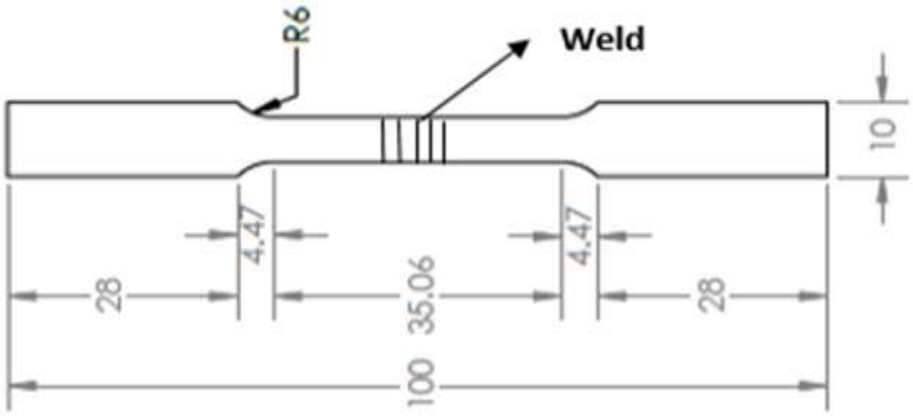

Figure 3.17: Tensile test specimen

Figure 3.18: Hounsfield Tensometer with specimen

Table 3.2: Tensile test parameters.

Speed (mm/min)	Extension range (mm)	Load range (kN)	Load cell (kN)
3	0-10	0-10	50

3.4.2. Bending Test

Prior to the performance of the bending test, the specimens were cut from different locations of the welded plate. Six of 20 mm X 140 mm rectangular shape specimems were cut perperndicular to the weld joint. Three were for the face test (that is the welded side of the plate) and onother three for the root test (which is underneath the welded side) as shown in figures 3. 19 and 3 20. The wire cutter machine was used to cut these specimens. Three-point bend tests as shown in figure 3.21 were conducted on the specimens using the same testing machine used for the tension tests. The machine parameters used were the same as the ones used for tension test. The data was logged and processed to produce the results that are presented in the next chapter.

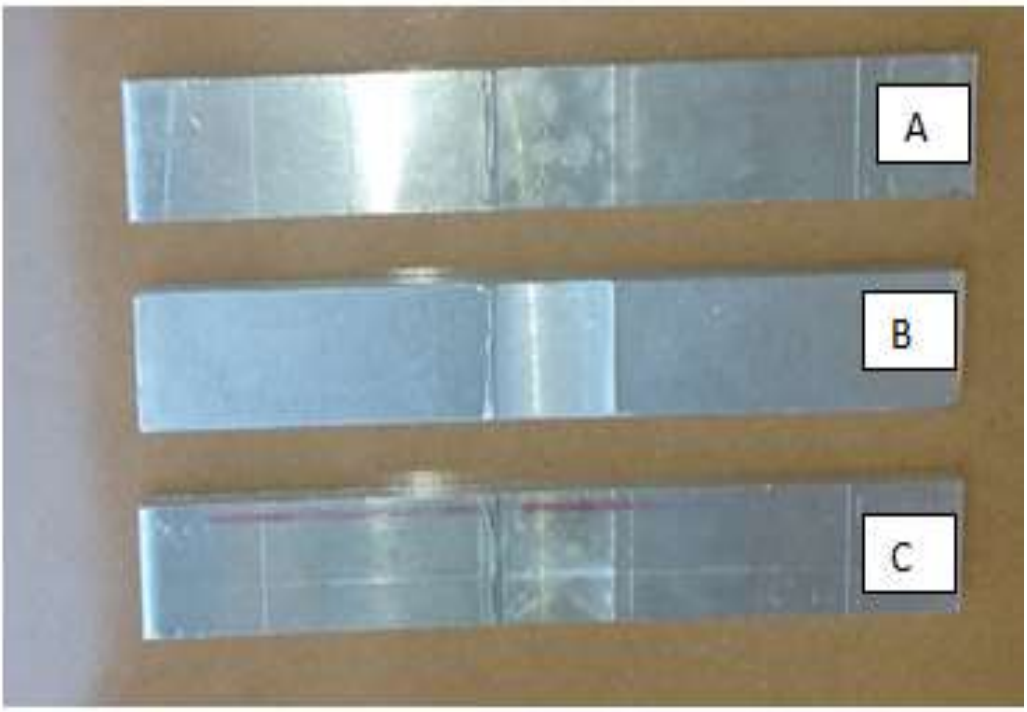

Figure 3.19: bending specimens (face)

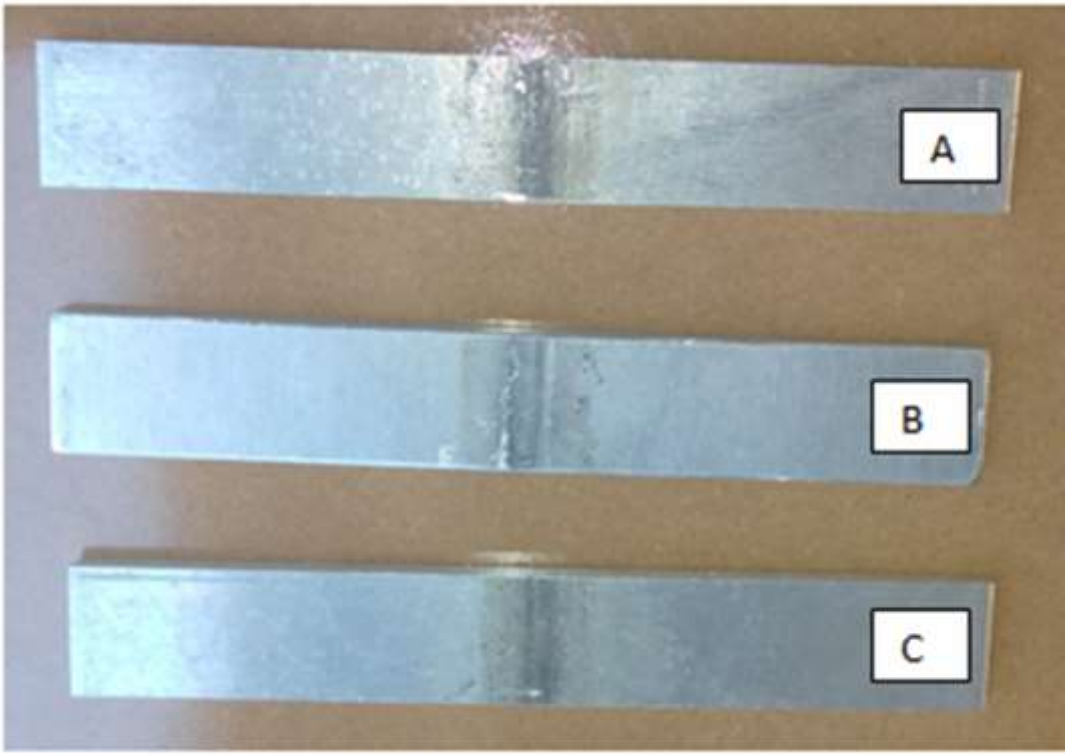

Figure 3.20: bending specimens (root)

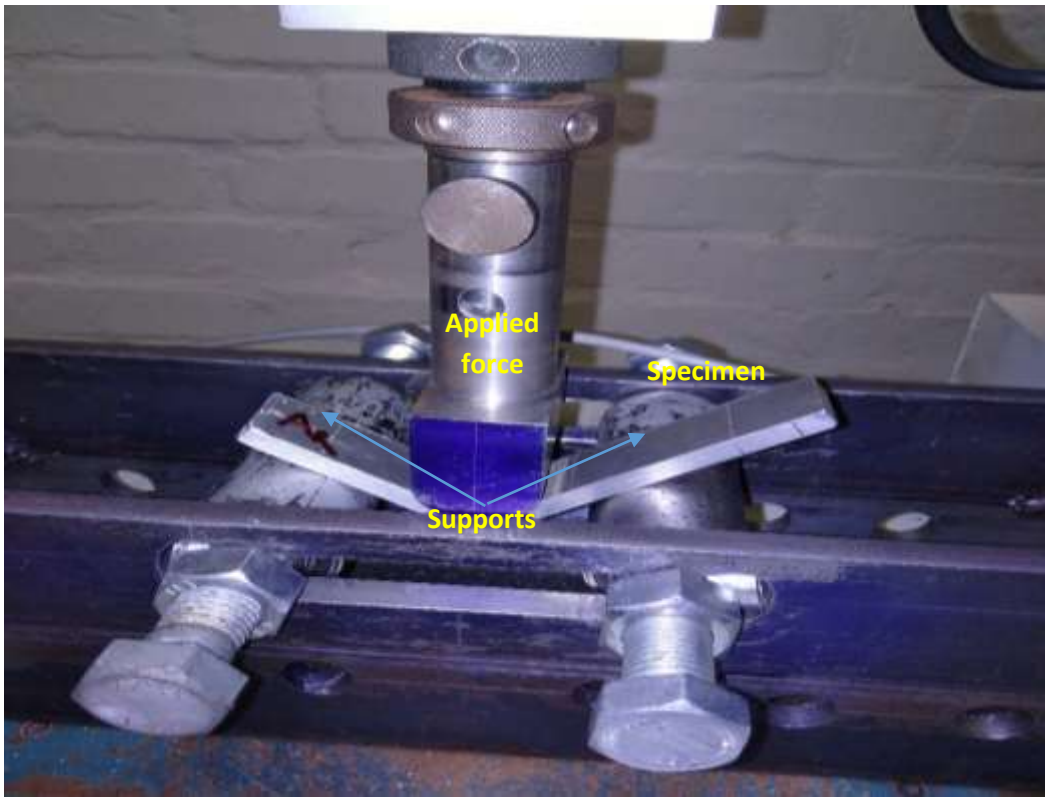

Figure 3.21: Bending test

3.4.3. Microstructure Analysis

Prior to the analysis of microstructure, the specimens were cut into 26 x 8 x 6 mm also from different location. The wire cutter machine was used to cut the specimens. The specimens were hot mounted using Struers labopress-3 machine. The mounted specimens were then polished to remove surface damage produced during cutting. The polished specimens were then etched using Keller's reagents shown in table 3.4. The procedure followed in polishing is summarized in Table 3.3. Fully prepared specimen is shown in figure 3.22. Nikon Eclipse L150 microscope was used for microstructural analysis. The microstructure was observed under polarized slider with an Axiocam 105 colour camera for acquiring the pictures.

Table 3.3: Disc grade, speed and chemicals used for polishing

Disk grade	Medium	Speed	Duration
Rhaco Grit P320	Distilled water	300 rpm	Until plane
Largan 9	DiaMaxx Poly 6µm	150 rpm	05:00 min
Moran- U	DiaMaxx Poly 3µm	150 rpm	04:00 min
Chemal	Fumed Silica 0.2µm Alkaline	150rpm	02:00 min

Table 3.4: Keller's reagent etchant

Solution	Quantity
Distilled water ($\boldsymbol{H_2O}$)	95 ml
Hydrochloric acid ($\boldsymbol{HCl}$)	1.5 ml
Hydrofluoric acid ($\boldsymbol{HF}$)	1.0 ml
Nitric acid ($\boldsymbol{HNO_3}$)	2.5 ml

Figure 3.22: Fully prepared specimens.

3.4.4. Scanning electron microscope (SEM)

It should be noted that SEM was outsourced. Tensile test fractured surfaces were cut to the sizes suitable for the SEM machine. The fractured surfaces were examined to investigate the nature of fracture.

CHAPTER FOUR

RESULTS AND DISCUSSIONS

The detailed discussions of the results obtained from the various test performed are presented in this section. The results obtained include the tensile test, bending test, microstructure and SEM analysis

4.1. Tensile test

The tensile test was performed on the specimens until they broke. Figure 4.1 shows the fractured specimens post tensile tests. It was observed that the fracture occurred on the advancing side (AA1050) of the specimen. Tensile test specimens fractured on the HAZ of the weaker material. This behaviour is also reported in literature [Ilangovan et al., 2015; Silva et al., 2011; Guo et al., 2014]. This behaviour suggests that the weld joint is mechanically stronger than the AA1050 parent material. This also suggests that the joint was dominated by a stronger material in our case its AA5083 alloy.

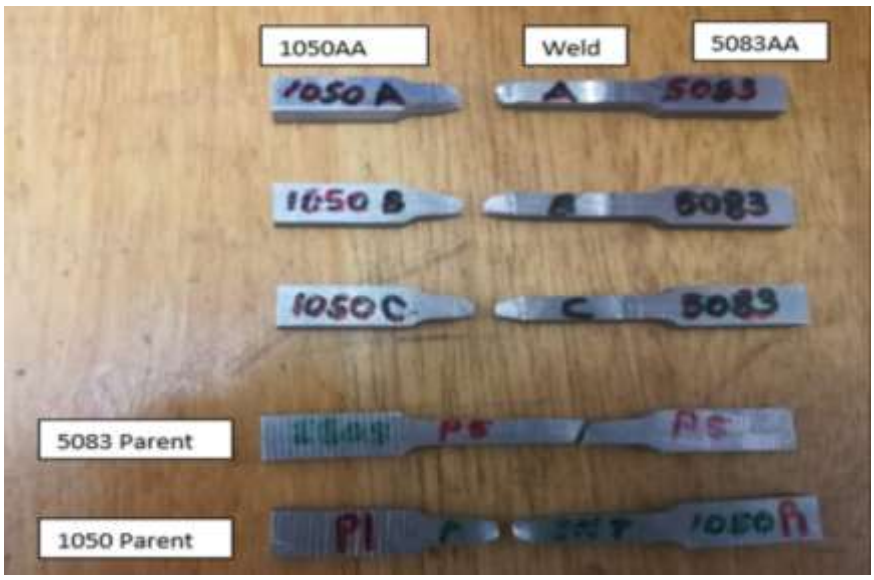

Figure 4.1: Tensile test fractured specimens

Table 4.1 shows the results of the ultimate tensile stress (UTS), tensile strain and percentage elongation. Specimen A was found to be the weakest specimen compared to the

other two. AA1050 and AA5083 show the UTS of 104.89 MPa and 326.75 MPa respectively, while the FSW specimen A, B and C shows 50.67 MPa, 66.47 MPa and 63.19 MPa respectively. The fracture occurred on the AA1050 side past the welding joint on the HAZ region. The UTS for the welds were all lower than the UTS for parent material and this behavior is similar to the one reported in the literature [Khodir & Shibayanagi, 2008; Ilangovan et al., 2015; Yadav, 2015]. The percentage of elongation of AA5083 parent material is higher than all the specimens. The welds have higher percentage elongation compared to the AA1050 parent material. This indicates that AA5083 is more ductile compared to all other specimens while AA1050 has the lowest ductility amongst the specimens [Brink & Maraschin, 2007].

Table 4.1: Tensile test results

Specimen	Ultimate Tensile strength (UTS) (MPa)	Tensile Strain	% elongation
A	50.67	0.075	7.5%
B	66.47	0.113	11.3%
C	63.19	0.116	11.6%
1050 Parent	104.89	0.066	6.6%
5083 Parent	326.75	0.263	26.3%

Figure 4.2 shows the tensile test-strain curve of AA1050, AA5083 and FSW specimens A, B and C. It is evident that the UTS of the parent material AA5083 is larger than that of the parent material AA1050 and of the FSW specimens. The stress-strain curve for specimen A is lower than all the curves. The curves for specimens B and C are very close to each other but lower than the parent materials. This behaviour is assumed to be caused by insufficient input temperature at the beginning of the weld. The temperature stabilizes from the middle to the end of the plate hence higher curves for specimens B and C.

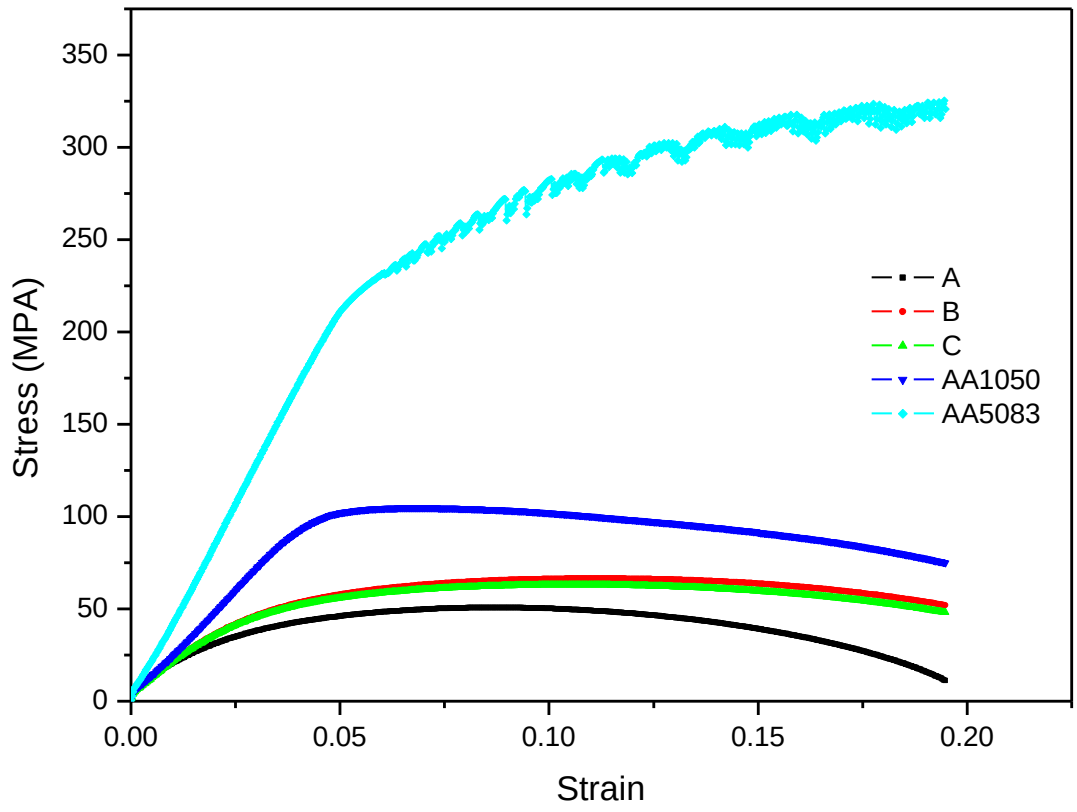

Figure 4.2: Tensile test – strain curves.

4.2. Bending Test

Figures 4.3 shows the post-test specimens for FSW where figure 4.3(a) represent face bent test and 4.3(b) shows root bend test. Figure 4.4 shows post-test specimens for base material of AA1050 and AA5083. The bending load was applied at the center of the specimens (red line) but the bending of all the specimens was on the side of AA1050. This means that the weldment was mechanically stronger compared to AA1050 hence bending occurred on the advancing side. This behaviour is in agreement with the behaviour observed in the tensile analysis [Ravikumar et al., 2013]. The friction stir welds presented good ductility, allowing for very high bend angles and no cracks were observed.

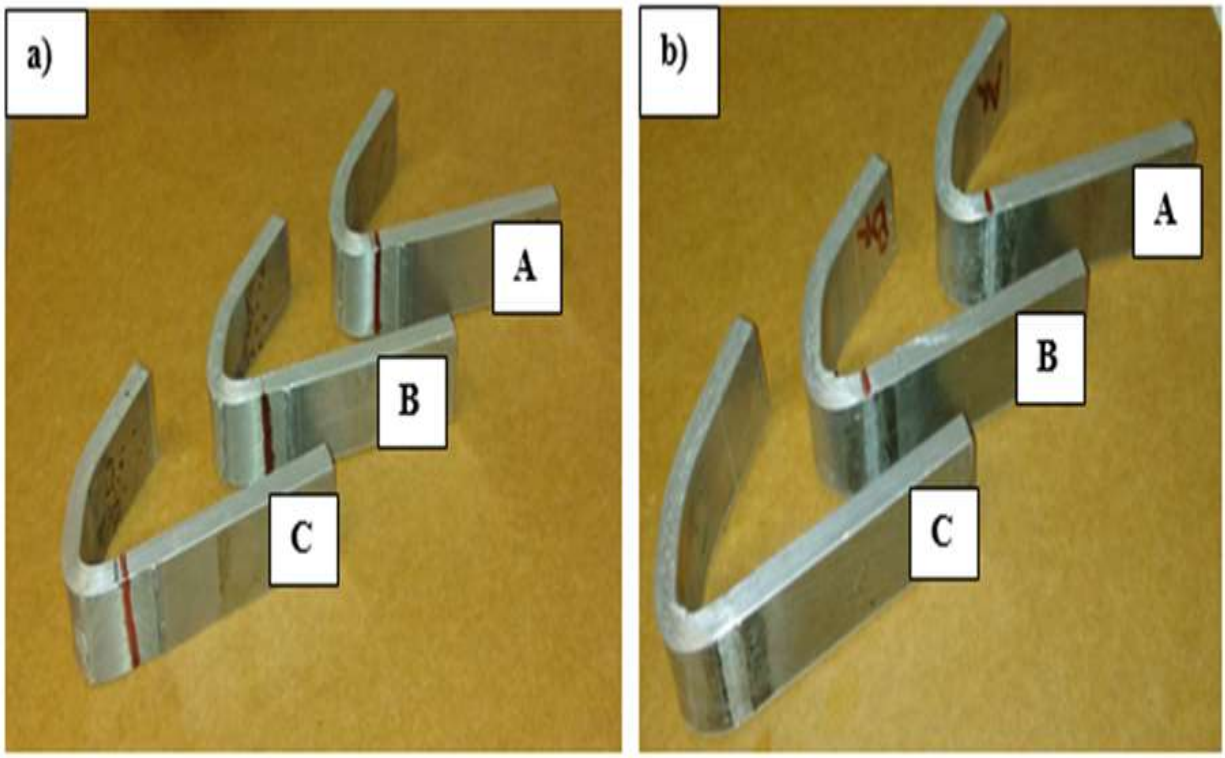

Figure 4.3: a) Tested bending specimen (face), b) Tested bending specimen (root)

Figure 4.4: Tested bending specimen (parent material)

Figures 4.5 and 4.6 shows bending stress and strain curves of friction stir welds together with parent materials. As it has been mentioned before that all the welded specimens bent

on AA1050, the flexural stresses for both face and root are within the range of that of AA1050 (see Table 4.2). The average stresses for face and root were 218.94MPa and 259MPa, respectively. Based on these results, the root side of the weld is stronger than that of the face. This is suggested to be caused by the fact that the lower side of the weld was exposed to a restricted downward movement due to the bed backing plate.

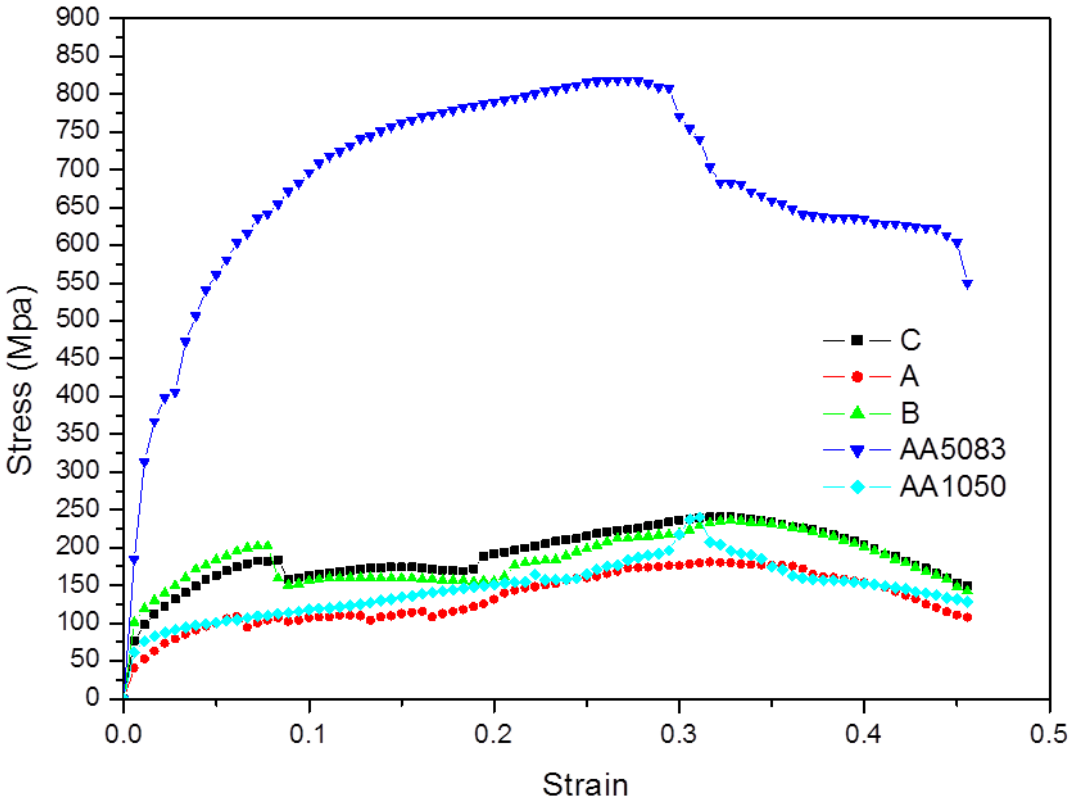

Figure 4.5: Bending stress-strain curves (face).

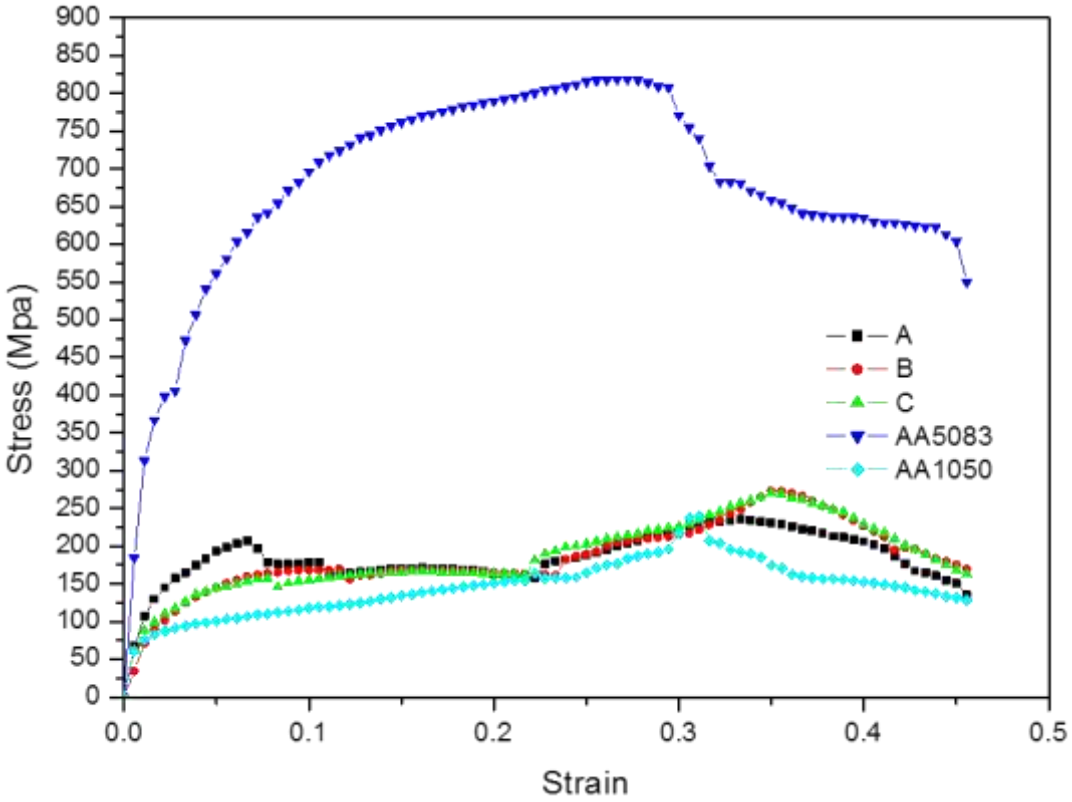

Figure 4.6: Bending stress-strain curves (root).

Table 4.2: Bending test results

Specimen	Flexural strength (MPa)	Flexural strain
Face		
A	240.56	0.32
B	180.38	0.31
C	235.88	0.33
Average stress	218.94	
Root		
A	234.75	0.33
B	272.25	0.35
C	270	0.35
Average stress	259	
Parent Materials		
AA1050	240.19	0.31
AA5083	818.44	0.27

4.3. Microstructure

The FSW joint is characterized by four different zones shown in figure 4.7. Those zones include weld nugget (WN) around the weld centre line, thermo-mechanically affected zone (TMAZ) on both sides of the weld nugget/stir zone, heat affected zone (HAZ) which is

surrounding the TMAZ, and non-affected base metal (BM) of AA1050 and AA5018. Recrystallization and microstructure evolution takes place during FSW and these changes are due to high plastic deformation and high temperature occurring in the stirred zone and this leads to precipitate dissolution and coarsening around the stir zone [Svensson et al., 2000]. There are no substantial changes in the base metal microstructure, though the weld nugget undergoes considerable amount of thermal changes. Figure 4.8-10 show the microstructural grains for the parent materials and the welded region. The grain size for the base metal AA1050 was ranging between 25 - 33µm while the grain size for AA5083 base metal ranged between 6.6 - 8µm. The grain size for the stir zone or welded region ranged between 7.3-11.4 µm. The grain size range for the stir zone is not far off from the grain size for AA5083 base metal. The morphology for the stir zone is similar to that of AA5083 base metal with some elongated whitish structures in between. These whitish elongated structures are suspected to be the trace of AA1050 which was pulled towards AA5083 during welding.

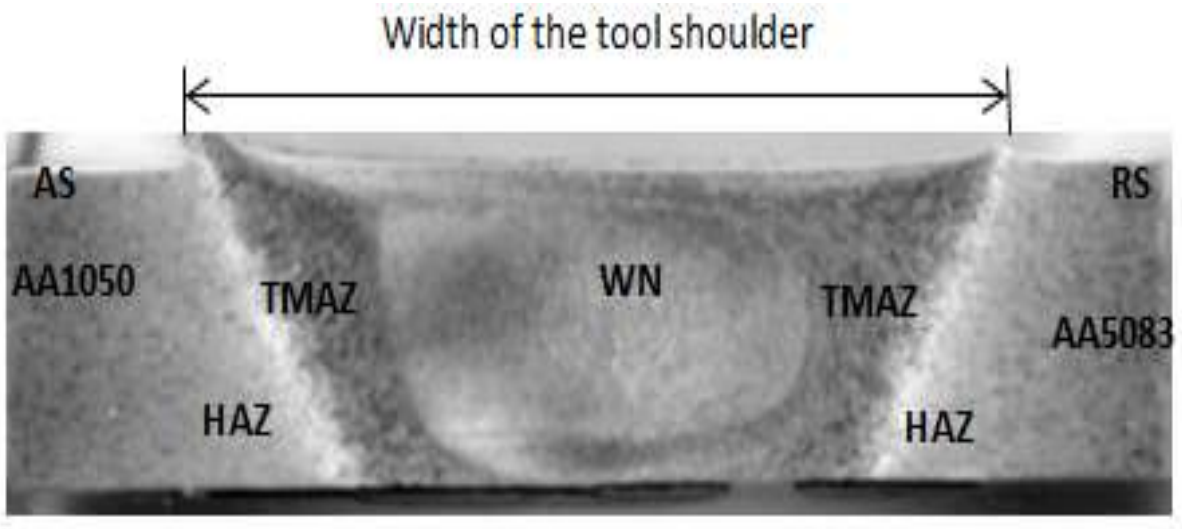

Figure 4.7: Macrostructure of the welded join as WN- weld nugget, TMAZ: thermo-mechanical affected zone, HAZ: heat affected zone.

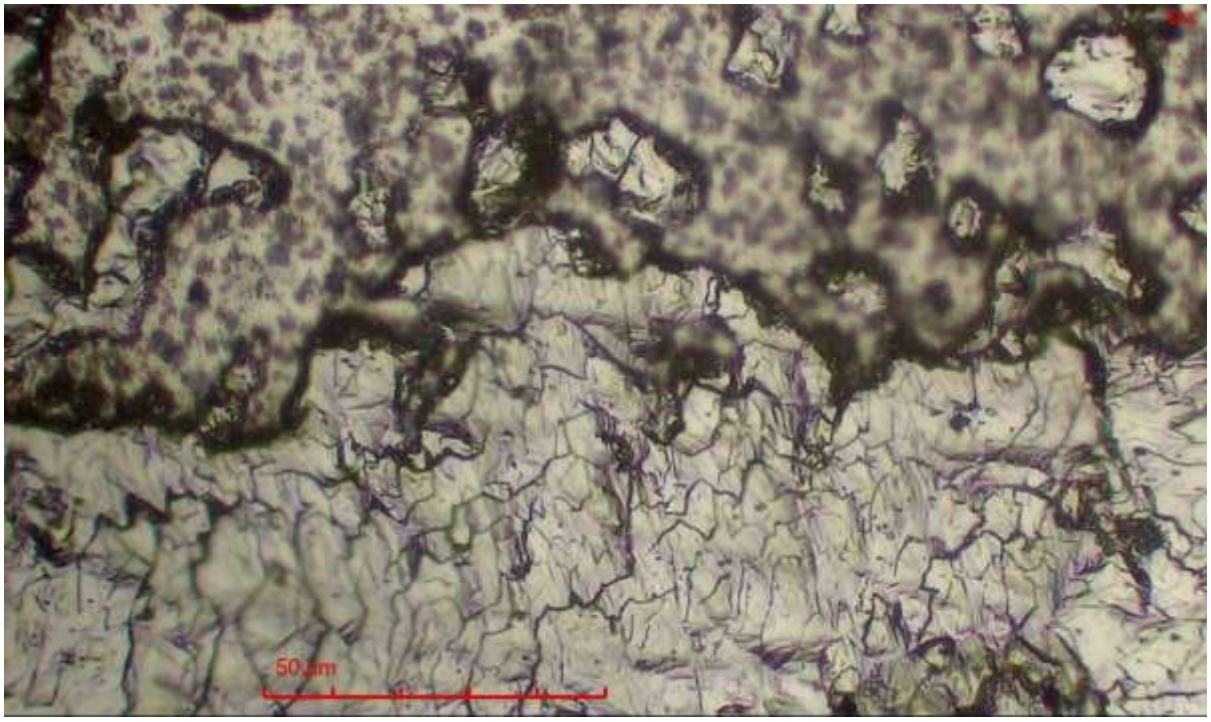

Figure 4.8: Micrograph for 1050 base metal

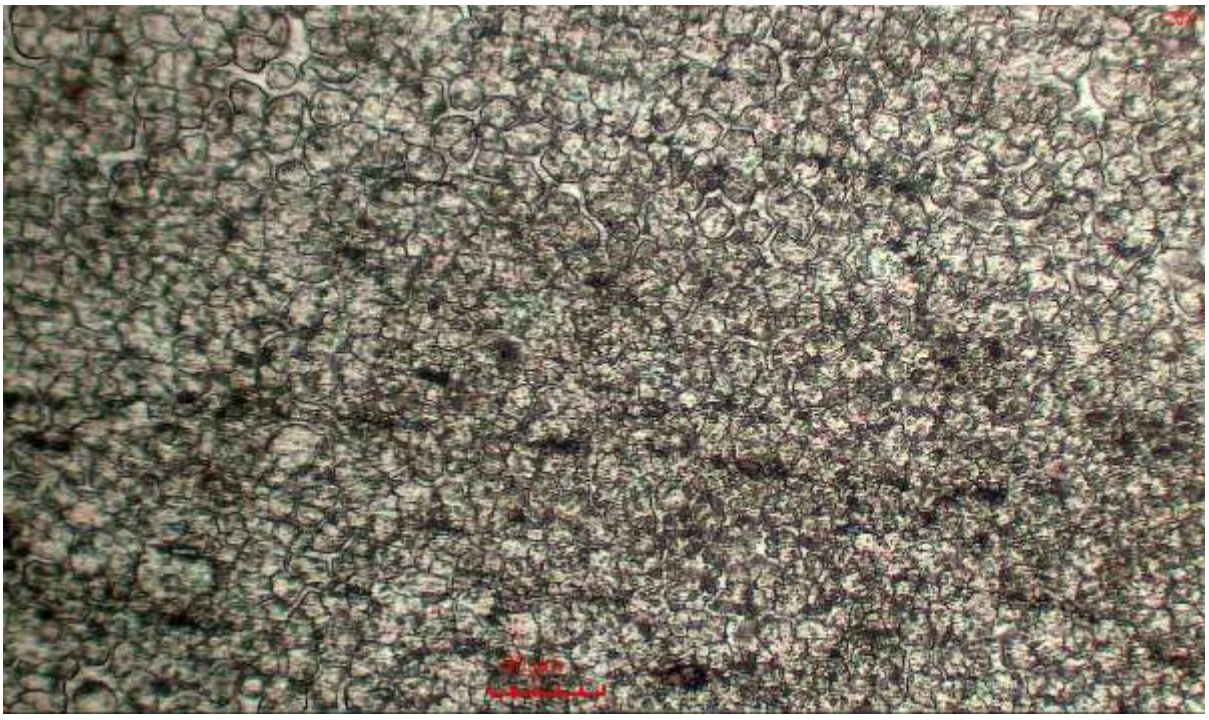

Figure 4.9: AA5083 base metal

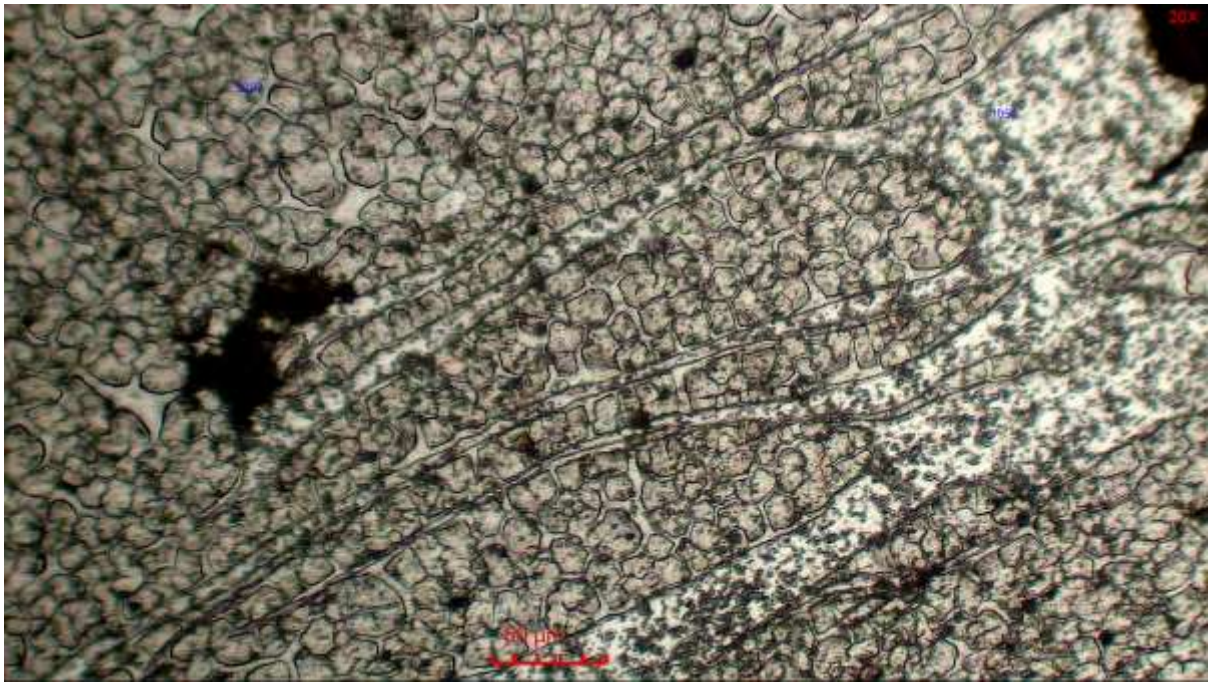

Figure 4.10: Micrograph for stir zone

4.4. Scanning electron microscope analysis

Figures 4.11 and 4.12 shows the fractured surface of tensile specimens that were analysed using SEM. It should be noted that the fractured surface for base metals were studied comparatively with specimen C. The elimination of other specimens was due to the fact that there was no distinction on the surface morphology for the other specimens. All the specimens show a cup like dimpled fracture which is a characterization of ductile failure mode [Ji et al., 2014]. The similarity in surface fracture suggests that the ductility of the materials involved in the joint formation was preserved post welding even though there were some percentage elongation variations.

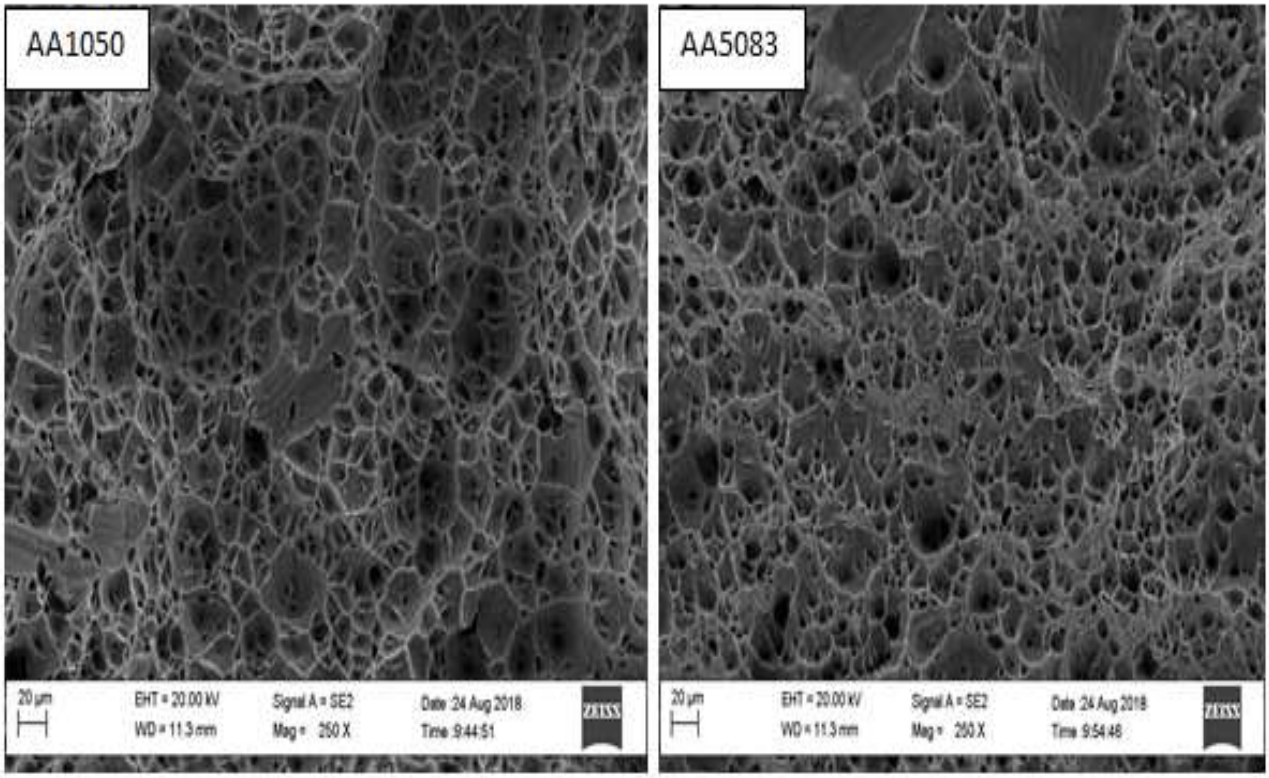

Figure 4.11: Micrograph of parent material

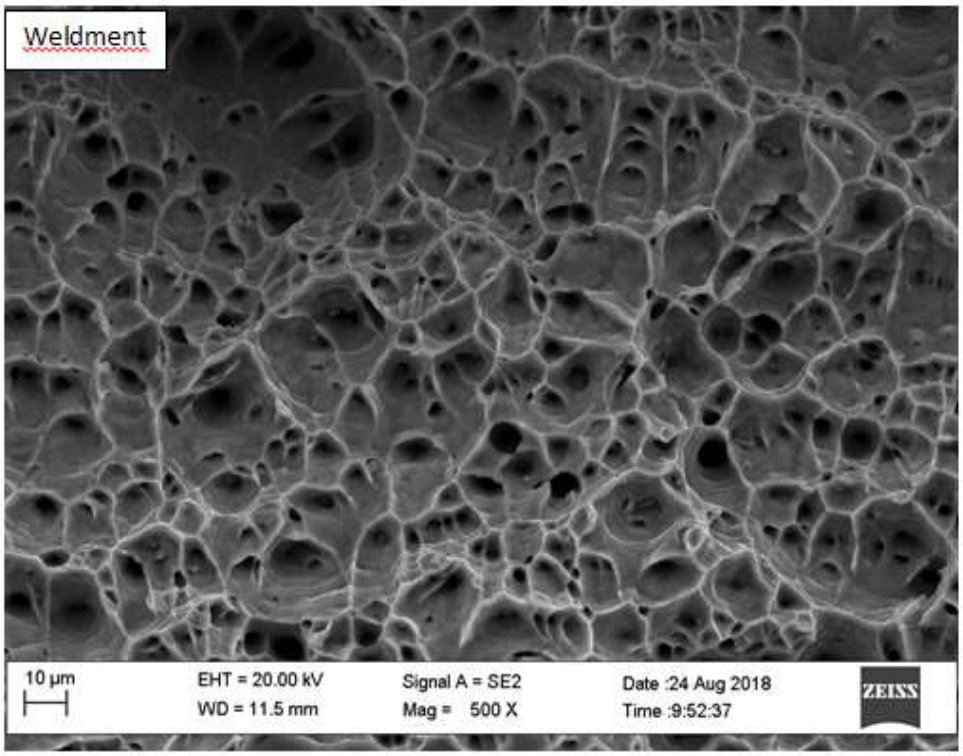

Figure 4.12: Micrograph of the welded specimen.

4.5 Microhardness

The microhardness profile for specimen C is presented in figure 4.13. The measurements were taken from the center to either side of the specimen. The measurements were conducted 3 mm from the root face of the specimen C. The microhardness of AA1050 base material is about 40 while the one for AA5083 base material ranges around 80. There is notable decrease in microhardness from the AA5083 side towards the center which then followed by the notable drastic increase towards the center of the weld. The graph also shows the slight decrease from the center towards the AA1050 side which then followed by gradual increase towards the end of the weld region. This behaviour is suggested to be caused by the variation in grain sizes because the increase in grain size reduces the value of the microhardness and the visa versa [Khodir & Shibayanagi, 2008].

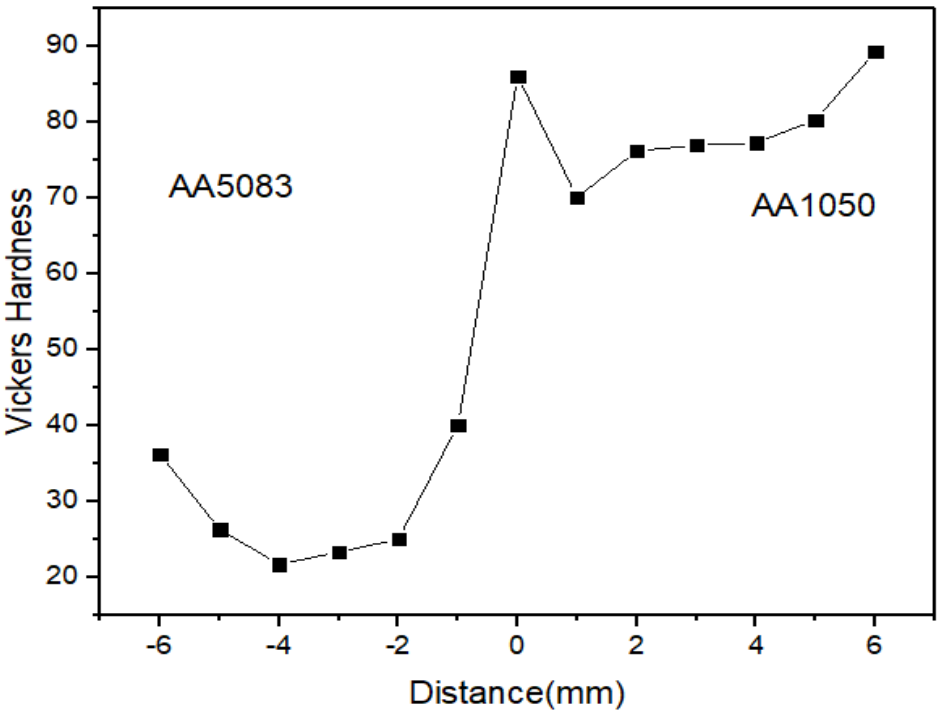

Figure 4.13: Microhardness

CHAPTER FIVE

CONCLUSION AND RECOMMENDATIONS

The study of mechanical properties of friction stir welded dissimilar aluminium alloys for the AA1050 and AA5083 plates were performed successfully. Prior to the performance of the welding, the high carbon steel was used in manufacturing the tool for welding. The FSW for this study was performed under uncontrolled environmental conditions. The preparation of welds analysis was performed using the equipment that does not impose heat during preparations hence the cutting was performed using wire cutter. There are number of analysis that were performed in order to understand the nature of the joint formed from these two dissimilar alloys i.e. AA1050 and AA5083. These tests include tensile test, bending test, microhardness test, SEM and microstructural analysis. Based on the analysis that were performed, the following conclusions were made:

Tensile tests were performed to the parent material and the joint until they fail. It was noted that all the welds specimens fractured on the HAZ of the AA1050. This behaviour suggest that the HAZ region for AA1050 was mechanically weaker compared to the joint formed. The mode of fracture was then analysed using SEM. The analysis revealed that the mode of fracture for the joints was ductile which was similar to the mode of fracture for the parent materials. This then suggests that the ductility of the joined materials was not affected post welding. There was a variation in grain size between AA1050 and AA5083 parent materials where AA1050 had higher grain sizes while AA5083 had smaller grain sizes. The joint formed show the grain size that are in the range similar to AA5083 parent material. This suggests that the welds were dominated by AA5083 material hence the fracture occurred on the AA1050 side. The percentage elongation for AA1050 parent material was found to be lower than all other specimens. This relates to the grain size of the material which has an influence on the microhardness of the material. The microhardness of the joint formed was found to be higher than the microhardness of the AA1050 parent material but at the same

range with AA5083. This correlates with the grain size range for the joint and the AA5083 parent material. The bending analysis showed that there was a good bond between the materials joined hence no trace of cracks post bending analysis. This suggests that the welding parameters used were suitable for welding these types of materials.

5.2. Recommendations for future work

The present work has provided the conclusion that FSW is a possible method to join dissimilar materials. The investigation giving support to this dissertation was focused on the aluminium alloy 1050 and 5083. The forthcoming investigations must be carried out using other relevant and light engineering materials such as polymeric materials. On the other hand, the technique of FSW in dissimilar materials could be improved, for instance, with the study of other geometries of the tool.

References

Ahmed, M.M.Z., Ataya, S., El-Sayed Seleman, M.M., Ammar, H.R. & Ahmed, E. 2017. Friction stir welding of similar and dissimilar AA7075 and AA5083. *Journal of Materials Processing Technology*, 242: 77–91.

Amancio-Filho, S.T., Sheikhi, S., dos Santos, J.F. & Bolfarini, C. 2008. Preliminary study on the microstructure and mechanical properties of dissimilar friction stir welds in aircraft aluminium alloys 2024-T351 and 6056-T4. *Journal of Materials Processing Technology*, 206(1–3): 132–142.

Andalucia, G. 2013. Aluminium Alloy 1050. : 1050.

Aval, H.J. & Kokabi, S.S.A.H. 2011. Thermo-mechanical and microstructural issues in dissimilar friction stir welding of AA5086 – AA6061. *Journal Material Science*, 46: 3258–3268.

Biswas, P. & Kumar, D.A. 2011. Friction stir welding of aluminum alloy with varying tool geometry and process parameters. *Journal of Engineering Manufacture*, 226(May 2014): 641–648.

Boşneag, A., Constantin, M.A., Niţu, E. & Iordache, M. 2017. Friction Stir Welding of three dissimilar aluminium alloy used in aeronautics industry. *IOP Conference Series: Materials Science and Engineering*, 252(1).

Brink, C; Maraschin, L. 2007. *Material Technology*. Heinemann publishers.

Cavaliere, P., Squillace, A. & Panella, F. 2007. Effect of welding parameters on mechanical and microstructural properties of AA6082 joints. , 0: 364–372.

Choi, D, H., Lee, C, Y., Ahn, B,W., Yeon, Y, M., Park, S, H, C., Sato, Y, S., Kokawa, H. & Jung, S, B. 2010. Effect of fixed location variation in friction stir welding of steels with different carbon contents. *Science and Technology of Welding and Joining*, 15: 299–

304.

Coelho, R.S., Kostka, A., Santos, J.F. & Kaysser-pyzalla, A. 2012. Materials Science & Engineering A Friction-stir dissimilar welding of aluminium alloy to high strength steels : Mechanical properties and their relation to microstructure. *Materials Science & Engineering A*, 556: 175–183.

Duong Dinh HaoTra ;Tran. 2015. Investigation of Effects of Friction Stir Welding Parameters on Bending Behavior of AA7075-T6. *International Journal of Engineering Research & Technology (IJERT)*, 4(9).

Ewuola, O.O., Akinlabi, E.T. & Madyira, D.M. 2015. Effect of Plunge Depth on Weld Integrity of Friction Stir Welds of Dissimilar Aluminium and Copper. : 1–4.

Farias, G. F. Batalha, E. F. Prados, R. & Magnabosco, S,D. 2013. Tool wear evaluations in friction stir processing of commercial titanium Ti-6Al-4V. , 302: 1327–1333.

Fazilah, N., Selamat, M., Sajuri, Z., Baghdadi, A.H. & Kokabi, A.H. 2016. Friction Stir Welding of Similar and Dissimilar Aluminium Alloys for Automotive Applications. *International Journal of Automotive and Mechanical Engineering*, 13(2): 3401–3412.

Genevois, C., Deschamps, A., Denquin, A. & Doisneau-Cottignies, B. 2005. Quantitative investigation of precipitation and mechanical behaviour for AA2024 friction stir welds. *Acta Materialia*, 53(8): 2447–2458.

Gharacheh, A. 2011. *Friction Stir Welding and Processing VI*. Canada: A John Wiley & Sons, Inc., Publication.

Guo, J.F., Chen, H.C., Sun, C.N., Bi, G., Sun, Z. & Wei, J. 2014. Friction stir welding of dissimilar materials between AA6061 and AA7075 Al alloys effects of process parameters. *Materials and Design*, 56: 185–192.

Heidarzadeh, A., Khodaverdizadeh, H., Mahmoudi, A. & Nazari, E. 2012. Tensile behavior of

friction stir welded AA 6061-T4 aluminum alloy joints. *JOURNAL OF MATERIALS&DESIGN*, 37: 166–173. http://dx.doi.org/10.1016/j.matdes.2011.12.022.

Ilangovan, M., Boopathy, S.R. & Balasubramanian, V. 2015. ScienceDirect Effect of tool pin profile on microstructure and tensile properties of friction stir welded dissimilar AA 6061 e AA 5086 aluminium alloy joints. *Defence Technology*, 11(2): 174–184. http://dx.doi.org/10.1016/j.dt.2015.01.004.

Ji, S.D., Meng, X.C., Liu, J.G., Zhang, L.G. & Gao, S.S. 2014. Formation and mechanical properties of stationary shoulder friction stir welded 6005A-T6 aluminum alloy. , 62: 113–117.

Joint, A.B. 2016. Joint, A.B. 2016. Effect of Friction Stir Welding Parameters on the Mechanical and Microstructure Properties of the.Effect of Friction Stir Welding Parameters on the Mechanical and Microstructure Properties of the.

Khodir, S.A. & Shibayanagi, T. 2008. Friction stir welding of dissimilar AA2024 and AA7075 aluminum alloys. *Materials Science & Engineering B*, 148: 82–87.

Klob, D., Kosec, L., Pietras, A. & Smolej, A. 2012. FRICTION-STIR WELDING OF ALUMINIUM ALLOY 5083. , 46(5): 483–488.

Kopyściański, M., Węglowska, A., Pietras, A., Hamilton, C. & Dymek, S. 2016. Friction Stir Welding of Dissimilar Aluminum Alloys Friction Stir Welding of Dissimilar Aluminum Alloys. , (February): 1–8.

Kostrivas A, L.J. 1999. Weldability of Li-bearing aluminium alloys. *International Materials Reviews*, 44: 217.

Kumar, K and Kaila, S. V. 2010. Positional dependence of material flow in friction stir welding – an analysis of joint line remnant and its relevance to dissimilar metal welding. *Science and Technology of Welding and Joining*, 15: 305–311.

Kumbhar, N.T. & Bhanumurthy, K. 2012. Friction Stir Welding of Al 5052 with Al 6061 Alloys. *Journal of Metallurgy*, 2012.

Kundu, J. & Singh, H. 2016. Friction stir welding of dissimilar Al alloys : Effect of process parameters on mechanical properties Friction stir welding of dissimilar Al alloys : effect of process parameters on mechanical properties. , (January).

Lim, S., Lee, C. & Kim, S. 2004. Tensile Behavior of Friction-Stir-Welded Al 6061-T651. , 35(September): 2829–2835.

Mathers, G. 2002. *The welding of aluminium and its aloys*. North America: Woodhead Publishing.

Meshram, M.P. Kodli, B.K. and S.R.D. 2014. "Friction Stir Welding of Austenitic Stainless Steel by PCBN Tool and its Joint Analyses. *Procedia Mater. Sci*, 6: 135–139.

Mishra, R.S. & Ma, Z.Y. 2005. Friction stir welding and processing. *Materials Science and Engineering*, 50(1–2): 1–78.

Mishra, R.S. & Mahoney, M.W. 2007. Friction Stir Welding and Processing. *ASM International*: 368.

Moreira, P.M.G.P., Santos, T., Tavares, S.M.O., Richter-trummer, V., Vilaça, P. & Castro, P.M.S.T. De. 2009. Mechanical and metallurgical characterization of friction stir welding joints of AA6061-T6 with AA6082-T6. , 30: 180–187.

Niu, P.L., Li, W.Y. & Chen, D.L. 2018. Strain hardening behavior and mechanisms of friction stir welded dissimilar joints of aluminum alloys. , 231: 68–71.

Ranjith, R. & Senthil Kumar, B. 2014. Joining of dissimilar aluminium alloys AA2014 T651 and AA6063 T651 by friction stir welding process. , 9: 179–186.

Ravikumar, S., Rao, V.S. & Ranjan, A. 2013. Evaluation of bending strength for Dissimilar Friction stir welded AA6061T651 - AA7075 T651 aluminium alloy butt joint. : 15–18.

Rhodes, C.G., Mahoney, M.W., Bingel, W.H., Spurling, R.A. & Bampton, C.C. 1997. Effects of friction stir welding on microstructure of 7075 aluminum. *Scripta Materialia*, 36(1): 69–75.

Rodriguez, R.I., Jordon, J.B., Allison, P.G., Rushing, T. & Garcia, L. 2015. Materials & Design Microstructure and mechanical properties of dissimilar friction stir welding of 6061-to-7050 aluminum alloys. *Materials & Design*, 83: 60–65. http://dx.doi.org/10.1016/j.matdes.2015.05.074.

Sadeesh, P., M, V.K., Rajkumar, V., Avinash, P., Arivazhagan, N., Ramkumar, K. & Narayanan, S. 2014. Studies on friction stir welding of AA 2024 and AA 6061 dissimilar metals. *Procedia Engineering*, 75: 145–149. http://dx.doi.org/10.1016/j.proeng.2013.11.031.

Sarsılmaz, F., Ozdemir, N. & Kırık, I. 2012. Evaluation of microstructure and fatigue properties of dissimilar AA7075 / AA6061 joints produced by friction stir welding. *Kovove Mater.*, 50: 259–268.

Sengar, S.S and Kuma, J. 2012. A study of recent trends in friction stir welding. : 646–649.

Serio, L.M., Palumbo, D., Alberto, L., Filippis, C. De, Galietti, U. & Ludovico, A.D. 2016. Effect of Friction Stir Process Parameters on the Mechanical and Thermal Behavior of 5754-H111 Aluminum Plates. *materials*, 9(122).

Silva, A.A.M., Arruti, E., Janeiro, G., Aldanondo, E., Alvarez, P. & Echeverria, A. 2011. Material flow and mechanical behaviour of dissimilar AA2024-T3 and AA7075-T6 aluminium alloys friction stir welds. *Materials and Design*, 32(4): 2021–2027. http://dx.doi.org/10.1016/j.matdes.2010.11.059.

V. Soundarajan, E. Yarrapareddy, R.K. 2007. Investigation of the friction stir lap welding of aluminium alloys AA 5182 and AA 6022. *Journal of Material Engineering and Performance*, 16(4): 477–484.

Sundaram, N.S. & Murugan, N. 2010. Tensile behavior of dissimilar friction stir welded joints of aluminium alloys. *Materials and Design*, 31(9): 4184–4193. http://dx.doi.org/10.1016/j.matdes.2010.04.035.

Svensson, L., Karlsson, L., Larsson, H., Karlsson, B., Fazzini, M. & Karlsson, J. 2000. Microstructure and mechanical properties of friction stir welded aluminium alloys with special reference to AA 5083 and AA 6082. *Science and Technology of Welding and Joining*, 5(5): 285–296.

Tang, W., Guo, X., McClure, J.C., Murr, L.E. & Nunes, A. 1998. Heat input and temperature distribution in friction stir welding. *Journal of Materials Processing and Manufacturing Science*, 7(2): 163–172.

Thimmaraju, P., Arkanti, K., Reddy, G.C. & Tilak, K.B.G. 2016. Comparison of Microstructure and Mechanical Properties of friction Stir welding of Al 6082 aluminum alloy with different Tool Profiles. *Materials Today: Proceedings*, 3(10): 4173–4181. http://dx.doi.org/10.1016/j.matpr.2016.11.092.

Thomas, B.W.M., Johnson, K.I. & Wiesner, C.S. 2003. Friction Stir Welding -Recent Developments in Tool and Process Technologies. , (7): 485–490.

Thomas, W.. & Nicholas, E.. 1997. Friction stir welding for the transportation industries. *Materials & Design*, 18(4–6): 269–273. http://linkinghub.elsevier.com/retrieve/pii/S0261306997000629.

Tiwari, S.K., Shukla, D.K. & Chandra, R. 2013. Friction Stir Welding of Aluminum Alloys : A Review. *International Journal of Mechanical, Aerospace, Industrial, Mechatronic and Manufacturing Engineering*, 7(12): 1326–1331.

Xia-wei, L.I., Da-tong, Z., Cheng, Q.I.U. & Wen, Z. 2012. Microstructure and mechanical properties of dissimilar pure copper / 1350 aluminum alloy butt joints by friction stir welding. *Transactions of Nonferrous Metals Society of China*, 22(6): 1298–1306.

http://dx.doi.org/10.1016/S1003-6326(11)61318-6.

Xu, W., Liu, J., Luan, G. & Dong, C. 2009. Microstructure and mechanical properties of friction stir welded joints in 2219-T6 aluminum alloy. *Materials and Design*, 30(9): 3460–3467. http://dx.doi.org/10.1016/j.matdes.2009.03.018.

Yadav, V.D. 2015. Friction Stir Welding of Dissimilar Aluminium alloys AA1100 to AA6101-T6. , (February).

Zhang, C., Huang, G., Cao, Y., Zhu, Y. & Liu, Q. 2019. On the microstructure and mechanical properties of similar and dissimilar AA7075 and AA2024 friction stir welding joints : Effect of rotational speed. *Journal of Manufacturing Processes*, 37(December 2018): 470–487. https://doi.org/10.1016/j.jmapro.2018.12.014.

Appendices

Appendix A: Base Plate

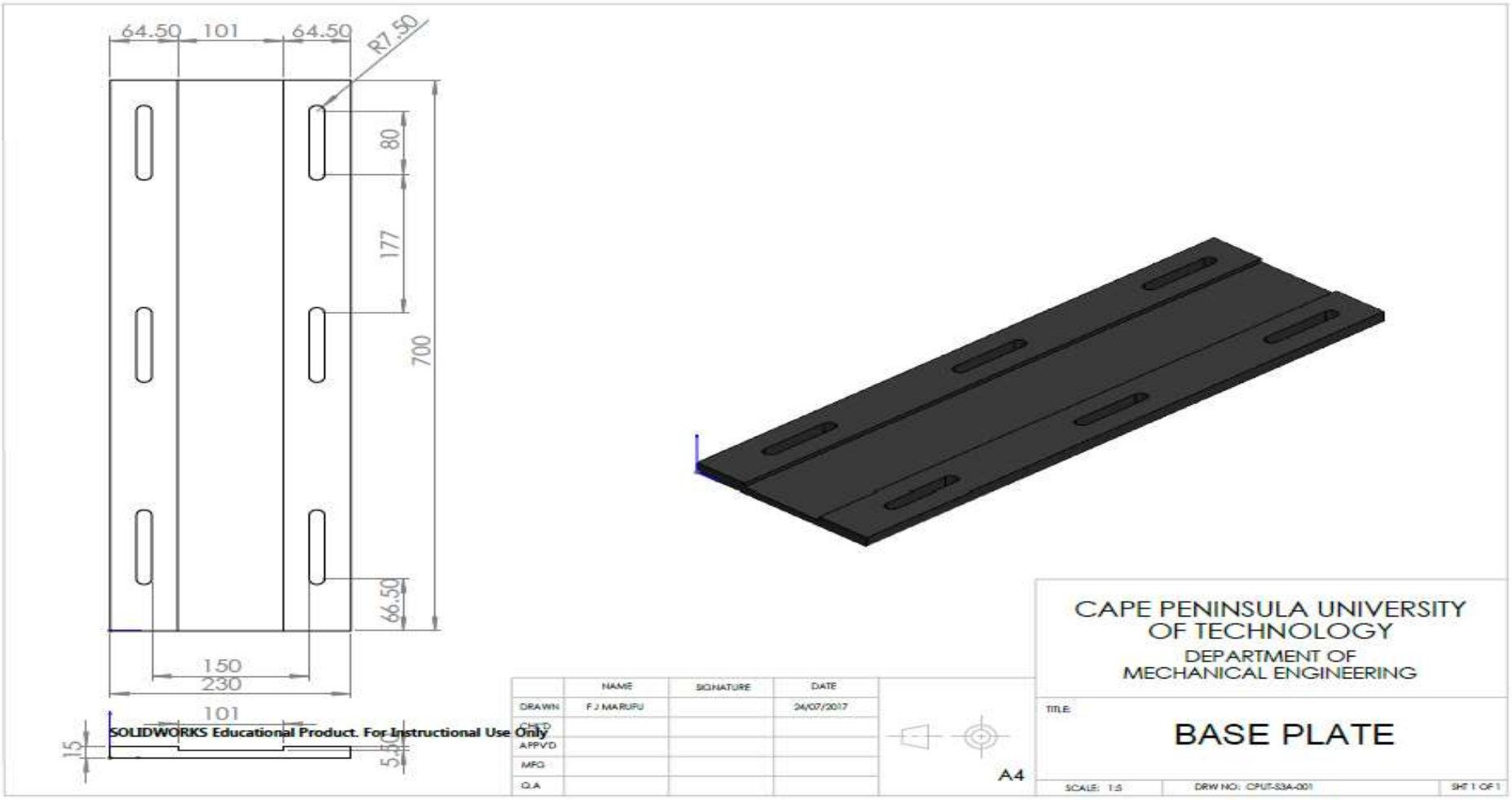

Appendix B: Clamps

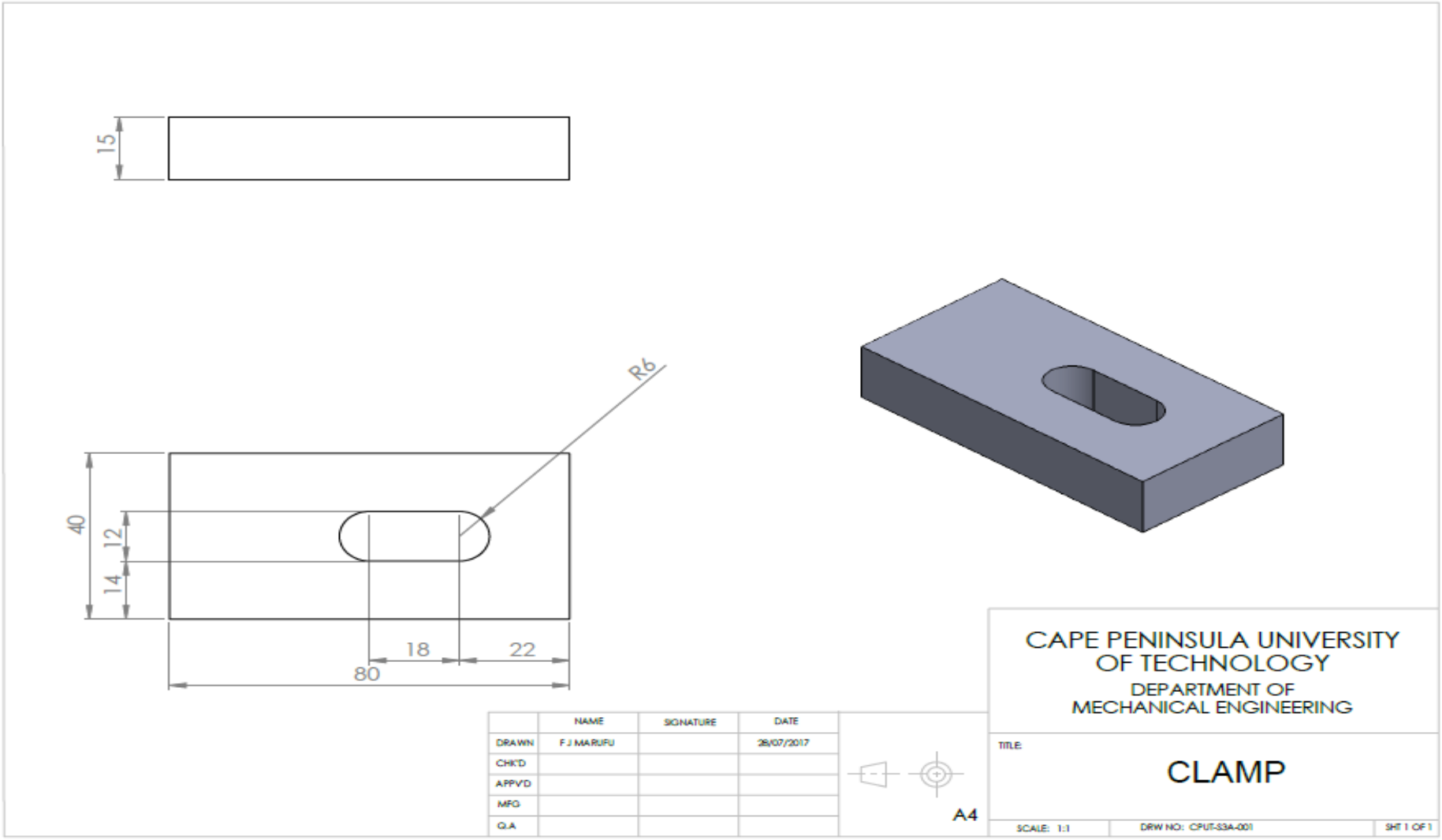

Appendix C: Tensile test specimen

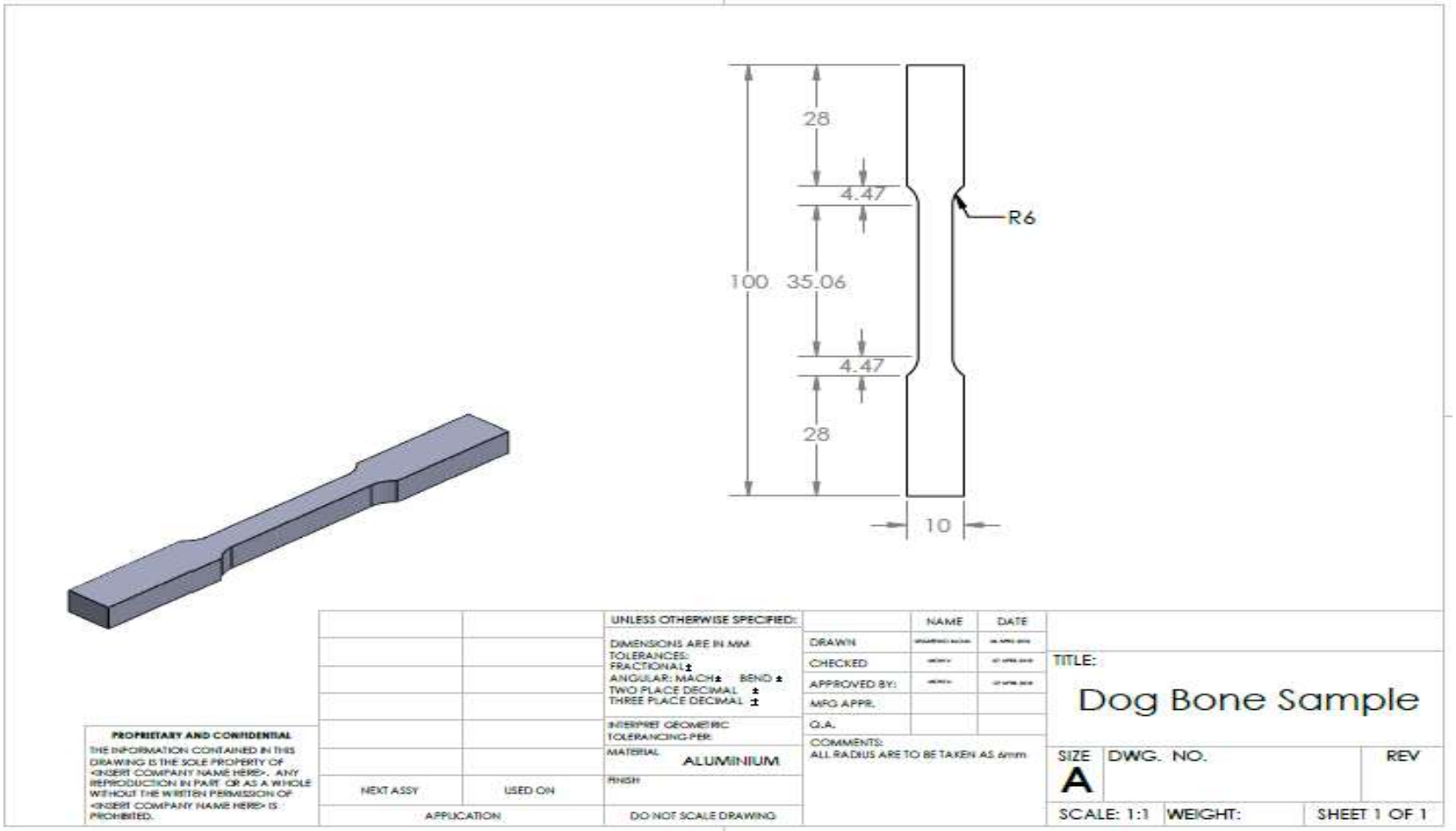

Appendix D: Sample calculations

Tensile test calculations

A) F=1824N, A=36mm^2

$$\sigma = \frac{F}{A} = \frac{1824}{0.000036}$$

$$= 50.67\ Mpa$$

$$\varepsilon = \frac{\Delta L}{L} = \frac{2.24}{30}$$

$$= 0.075$$

$$\%\ Elongation = \frac{\Delta L}{L} X100 = \frac{2.24}{30} X100 = 7.5\%$$

B) F=2393N, A= 36mm^2

$$\sigma = \frac{F}{A} = \frac{2393}{0.000036}$$

$$= 66.47\ Mpa$$

$$\varepsilon = \frac{\Delta L}{L} = \frac{3.4}{30}$$

$$= 0.113$$

$$\%\ Elongation = \frac{\Delta L}{L} X100 = \frac{3.4}{30} X100 = 11.3\%$$

C) F= 2275N, A= 36mm^2

$$\sigma = \frac{F}{A} = \frac{2275}{0.000036}$$

$$= 63.19\ Mpa$$

$$\varepsilon = \frac{\Delta L}{L} = \frac{3.48}{30}$$

$$= 0.116$$

$$\%\ Elongation = \frac{\Delta L}{L} X100 = \frac{3.48}{30} X100 = 11.6\%$$

Parent 1050 → F= 3776N, A=36mm^2 $\sigma = \frac{F}{A} = \frac{3776}{0.000036}$

$= 104.89\ Mpa$

$\varepsilon = \frac{\Delta L}{L} = \frac{1.980}{30}$

$= 0.066$

$\%\ Elongation = \frac{\Delta L}{L} X100 = \frac{1.980}{30} X100 = 6.6\%$

Parent 5083 → F=11763N, A=36mm^2 $\sigma = \frac{F}{A} = \frac{11763}{0.000036}$

$= 326.75\ Mpa$

$\varepsilon = \frac{\Delta L}{L} = \frac{7.9}{30}$

$= 0.263$

$\%\ Elongation = \frac{\Delta L}{L} X100 = \frac{7.9}{30} X100 = 26.3\%$

Bending test calculations

Face

$A)$ $\sigma = \frac{3FL}{2bd^2} = \frac{3X1283X90}{2X20X6^2}$

$= 240.56\ Mpa$

$\varepsilon = \frac{\Delta L}{L} = \frac{29}{90}$

=0.322

$B)$ $\sigma = \frac{3FL}{2bd^2} = \frac{3X962X90}{2X20X6^2}$

$= 180.38\ Mpa$

$\boldsymbol{\varepsilon = \frac{\Delta L}{L} = \frac{28.5}{90}}$

=0.317

$C)$ $\sigma = \frac{3FL}{2bd^2} = \frac{3X1258X90}{2X20X6^2}$

$= 235.88\ Mpa$

$\boldsymbol{\varepsilon = \frac{\Delta L}{L} = \frac{29.5}{90}}$

=0.328

Root

$A)$ $\sigma = \frac{3FL}{2bd^2} = \frac{3X1252X90}{2X20X6^2}$

$= 234.75\ Mpa$

$\varepsilon = \frac{\Delta L}{L} = \frac{30}{90}$

=0.333

B) $\sigma = \boldsymbol{\frac{3FL}{2bd^2}} = \frac{3X1452X90}{2X20X6^2}$

$= 272.25\ Mpa$

$\varepsilon = \frac{\Delta L}{L} = \frac{31.5}{90}$

=0.35

$C)$ $\sigma = \frac{3FL}{2bd^2} = \frac{3X1440X90}{2X20X6^2}$

$= 270\ Mpa$

$\varepsilon = \frac{\Delta L}{L} = \frac{31.5}{90}$

=0.35

For parent material

AA1050 $\sigma = \frac{3FL}{2bd^2} = \frac{3X1281X90}{2X20X6^2}$

$= 240.19\ Mpa$

$\varepsilon = \frac{\Delta L}{L} = \frac{28}{90}$

=0.31

AA5083 $\sigma = \frac{3FL}{2bd^2} = \frac{3X4365X90}{2X20X6^2}$

$= 818.44\ Mpa$

$\varepsilon = \frac{\Delta L}{L} = \frac{24.5}{90}$

=0.27